

Why do Green's functions?

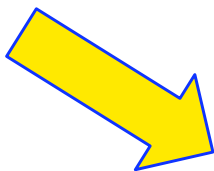
- Properly executed --> answers an old question from Sir Denys Wilkinson: "What does a nucleon do in the nucleus?"
- Nucleon self-energy → think of potential but energy dependent
- Nucleon self-energy → elastic nucleon scattering data --> input for the analysis of many nuclear reactions
- Nucleon self-energy → bound-state overlap functions with their normalization --> also used in the analysis of nuclear reactions --> for exotic nuclei only strongly interacting probes available
- Nucleon self-energy → density distribution & E/A from V_{NN}
- Self-energy <--> data --> dispersive optical model (DOM)



Location of single-particle strength in closed-shell (stable) nuclei

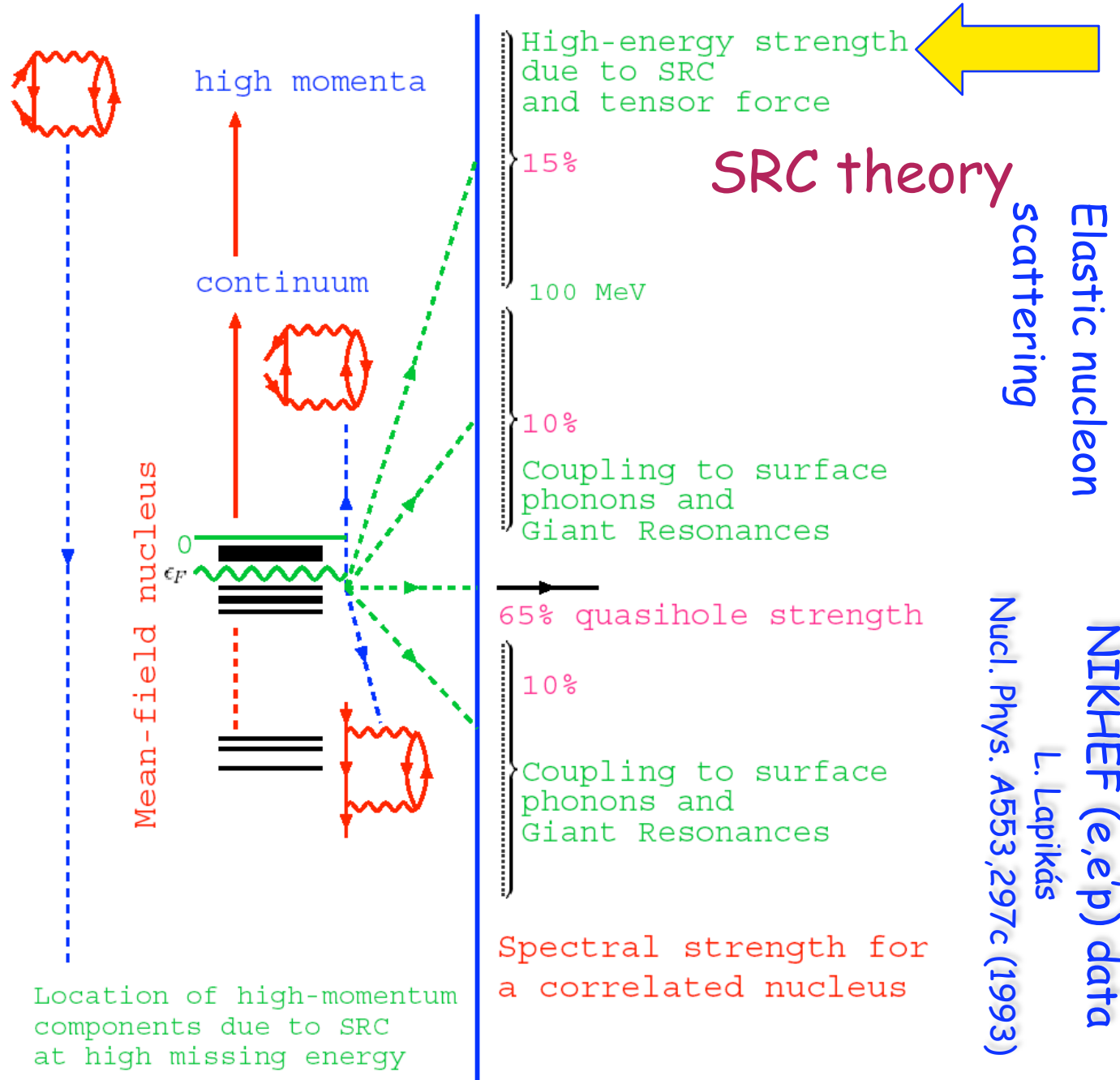
For example: protons in ^{208}Pb

SRC



JLab E97-006

Phys. Rev. Lett. 93, 182501 (2004) D. Rohe et al.



Remarks

- Given a Hamiltonian, a perturbation expansion can be generated for the single-particle propagator
- Dyson equation determines propagator in terms of nucleon self-energy
- Self-energy is causal and obeys dispersion relations relating its real and imaginary part
- Data constrained self-energy acts as ideal interface between ab initio theory and experiment

Propagator / Green's function

- Lehmann representation

$$G_{\ell j}(k, k'; E) = \sum_m \frac{\langle \Psi_0^A | a_{k\ell j} | \Psi_m^{A+1} \rangle \langle \Psi_m^{A+1} | a_{k'\ell j}^\dagger | \Psi_0^A \rangle}{E - (E_m^{A+1} - E_0^A) + i\eta} + \sum_n \frac{\langle \Psi_0^A | a_{k'\ell j}^\dagger | \Psi_n^{A-1} \rangle \langle \Psi_n^{A-1} | a_{k\ell j} | \Psi_0^A \rangle}{E - (E_0^A - E_n^{A-1}) - i\eta}$$

- Any other single-particle basis can be used

- Overlap functions --> numerator

- Corresponding eigenvalues --> denominator

- Spectral function

$$S_{\ell j}(k; E) = \frac{1}{\pi} \text{Im} G_{\ell j}(k, k; E) \quad E \leq \varepsilon_F^-$$

$$= \sum_n \left| \langle \Psi_n^{A-1} | a_{k\ell j} | \Psi_0^A \rangle \right|^2 \delta(E - (E_0^A - E_n^{A-1}))$$

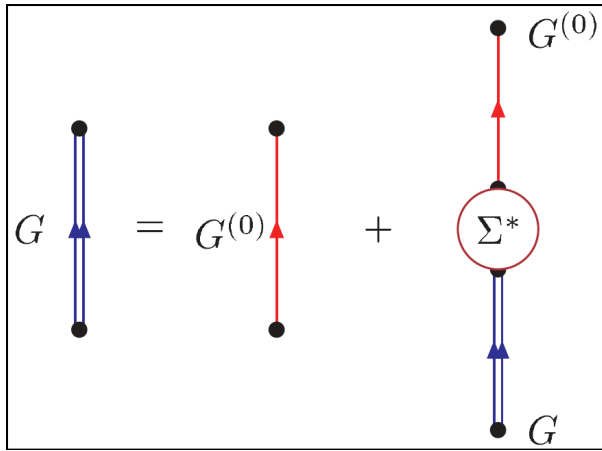
- Spectral strength in the continuum

$$S_{\ell j}(E) = \int_0^\infty dk k^2 S_{\ell j}(k; E)$$

- Discrete transitions $\sqrt{S_{\ell j}^n} \phi_{\ell j}^n(k) = \langle \Psi_n^{A-1} | a_{k\ell j} | \Psi_0^A \rangle$

- Positive energy → see later

Propagator from Dyson Equation and "experiment"



Equivalent to ...

Schrödinger-like equation with: $E_n^- = E_0^A - E_n^{A-1}$

Self-energy: non-local, energy-dependent potential

With energy dependence: spectroscopic factors < 1

⇒ as extracted from (e,e'p) reaction

$$\frac{k^2}{2m} \phi_{lj}^n(k) + \int dq q^2 \Sigma_{lj}^*(k, q; E_n^-) \phi_{lj}^n(q) = E_n^- \phi_{lj}^n(k)$$

Spectroscopic factor $S_{lj}^n = \int dk k^2 |\langle \Psi_n^{A-1} | a_{klj} | \Psi_0^A \rangle|^2 < 1$

Dyson equation also yields $[\chi_{lj}^{elE}(r)]^* = \langle \Psi_{elE}^{A+1} | a_{rlj}^\dagger | \Psi_0^A \rangle$ for positive energies



Elastic scattering wave function for protons or neutrons

Dyson equation therefore provides:

Link between scattering and structure data from **dispersion relations**

reactions and structure

How is it done in practice?

- Dyson equation for discrete states

$$\left[\frac{p_r^2}{2m} + \frac{\hbar^2 \ell(\ell+1)}{2mr^2} \right] \psi_{\ell j}^n(r) + \int dr' r'^2 \Sigma_{\ell j}(r, r'; \varepsilon_n^-) \psi_{\ell j}^n(r') = \varepsilon_n^- \psi_{\ell j}^n(r)$$

- with $p_r = -\frac{i}{\hbar} \left(\frac{\partial}{\partial r} + \frac{1}{r} \right)$

- Work with $u_{\ell j}^n(r) = r \psi_{\ell j}^n(r)$ so only 2nd derivative $\frac{d^2}{dr^2}$

- Put coordinate on equidistant grid $r_i = (i - 1/2)\Delta$ $i = 1, 2, \dots$

- Approximate 2nd derivative for $i > 1$ by

$$u''(r_i) = [u(r_{i+1}) + u(r_{i-1}) - 2u(r_i)] / \Delta^2$$

- First point $u''(r_1) = [u(r_2) + u(r_0) - 2u(r_1)] / \Delta^2$

- Use "continuity" for $r < 0$: for parity $\pm 1 \Rightarrow u(-r) = \pm u(r)$

- using bc \rightarrow
 $u''(r_1) = [u(r_2) - u(r_1)] / \delta^2 \Rightarrow +$
 $u''(r_1) = [u(r_2) - 3u(r_1)] / \delta^2 \Rightarrow -$ then diagonalize etc.

Propagator

- Same discretization

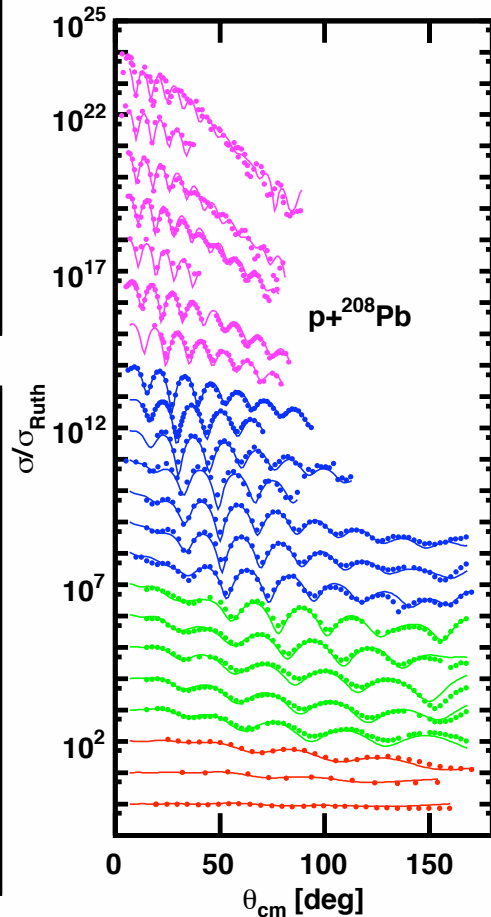
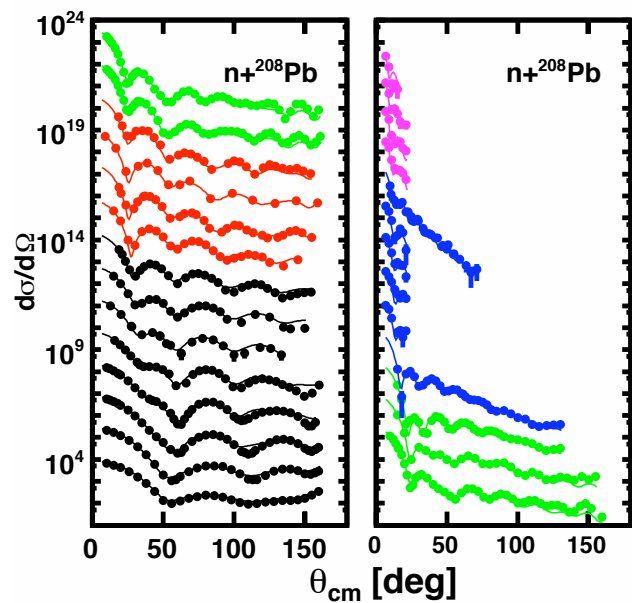
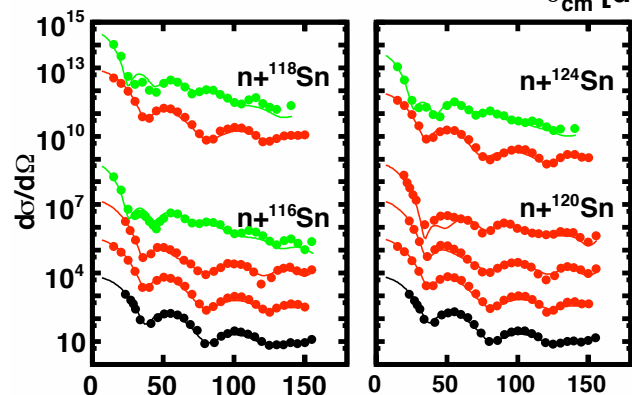
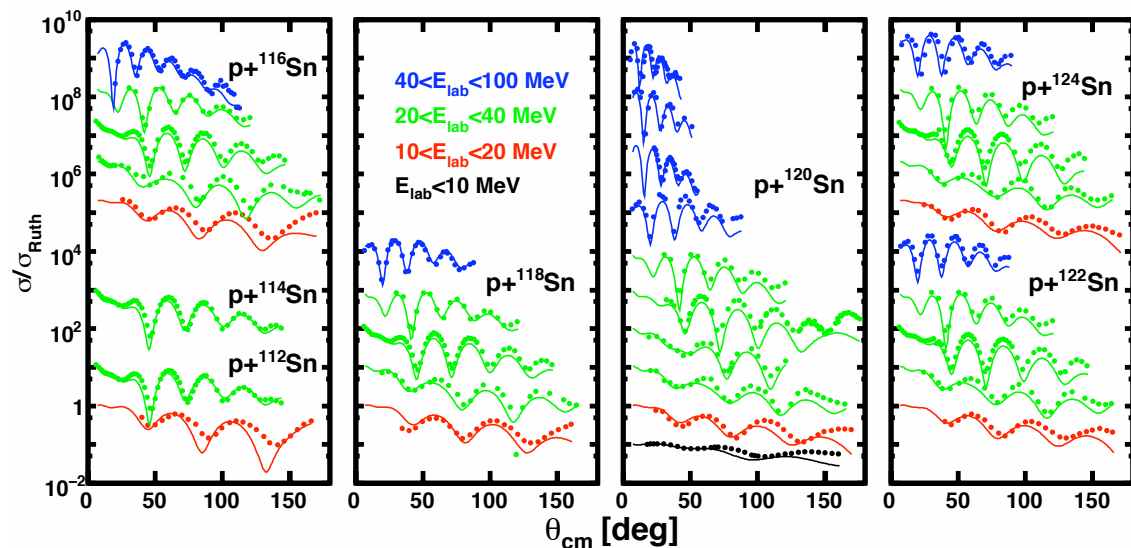
$$G_{\ell j}(r, r'; E) = G_{\ell j}^{(0)}(r, r'; E) + \int d\tilde{r} \tilde{r}^2 \int d\tilde{r}' \tilde{r}'^2 G_{\ell j}^{(0)}(r, \tilde{r}; E) \Sigma_{\ell j}(\tilde{r}, \tilde{r}'; E) G_{\ell j}(\tilde{r}', r'; E)$$

- Use matrix inversion now

- Then spectral amplitude $S_{\ell j}(r, r'; E) = \frac{1}{\pi} \text{Im} G_{\ell j}(r, r'; E)$

- Spectral function $S_{\ell j}(r; E) = \frac{1}{\pi} \text{Im} G_{\ell j}(r, r; E)$

- and so on

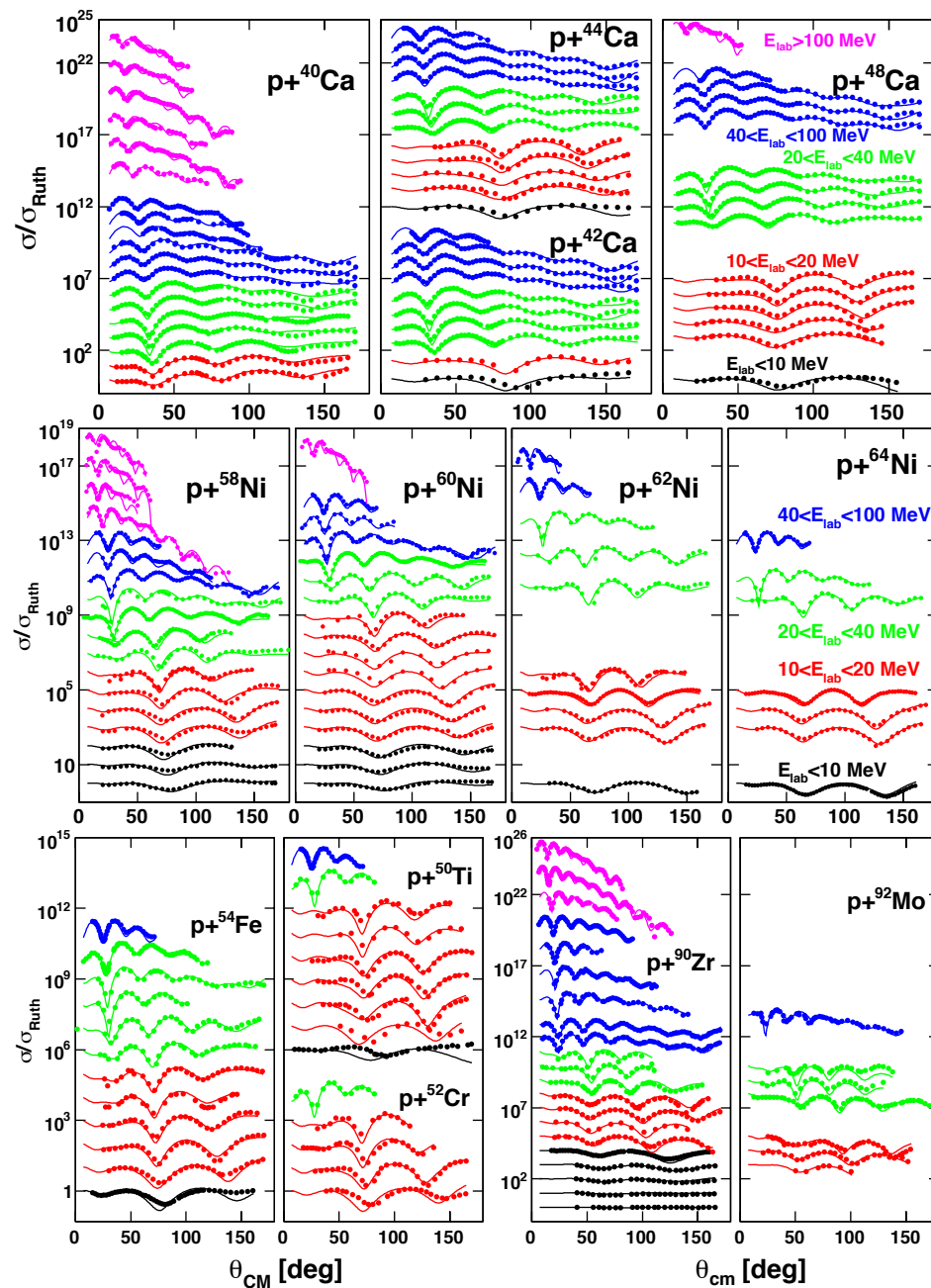
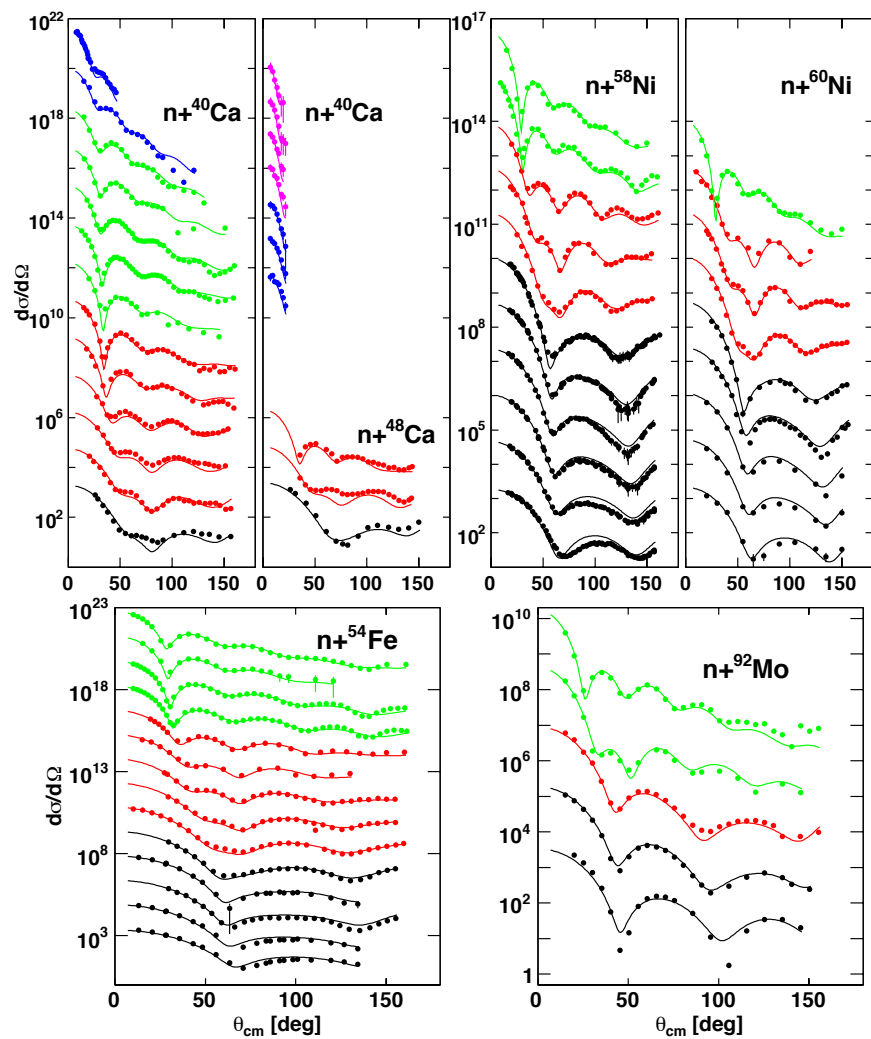


Recent local
DOM analysis
--> towards
global

J. Mueller et al.
PRC83,064605 (2011), 1-32

Elastic scattering data for protons and neutrons

- Abundant for stable targets

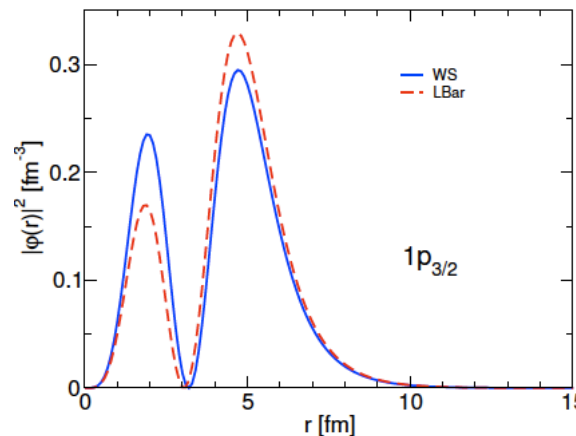
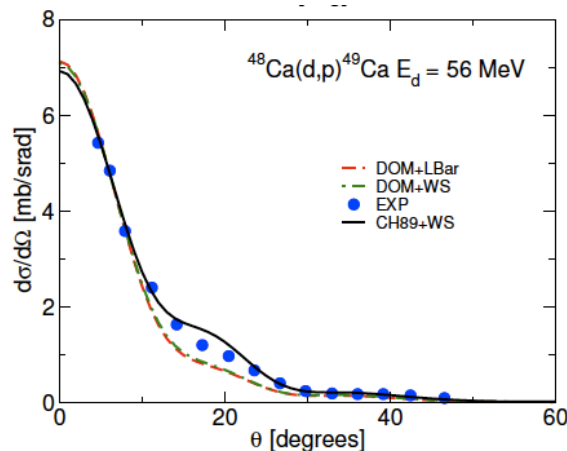
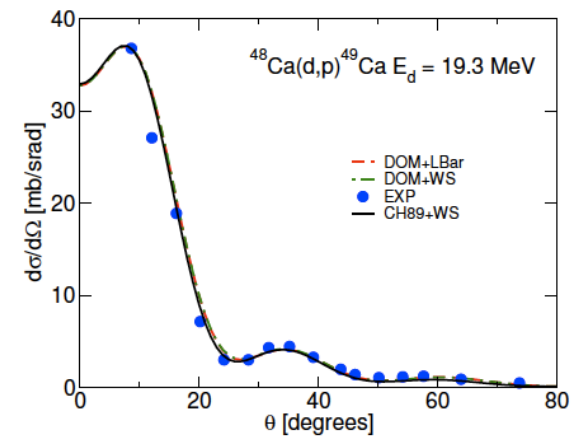
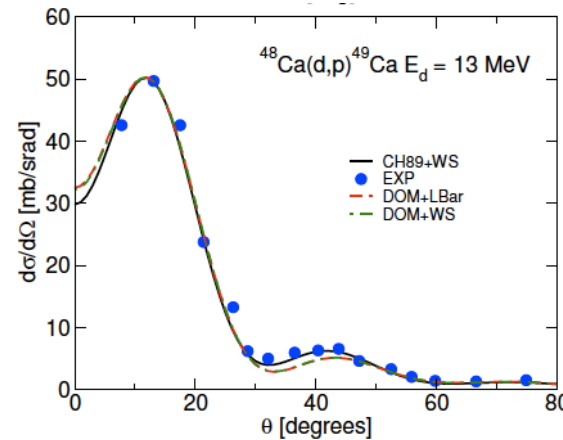
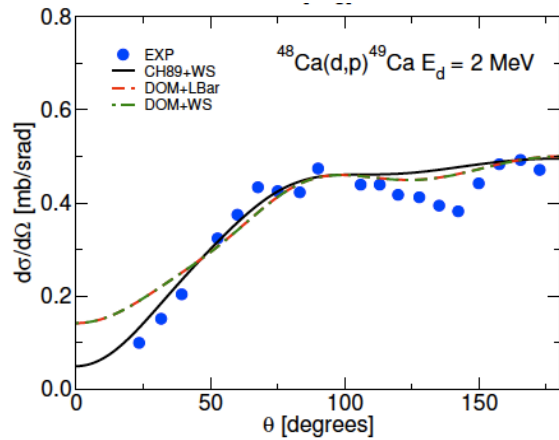


Local DOM ingredients and transfer reactions

- Overlap function
- p and n optical potential
- ADWA (developed by Ron Johnson)
- MSU-WashU:-->
- $^{40,48}\text{Ca}, ^{132}\text{Sn}, ^{208}\text{Pb}(d,p)$

N. B. Nguyen, S. J. Waldecker, F. M. Nuñez, R. J. Charity, and W. H. Dickhoff

[Phys. Rev. C84, 044611 \(2011\), 1-9](#)

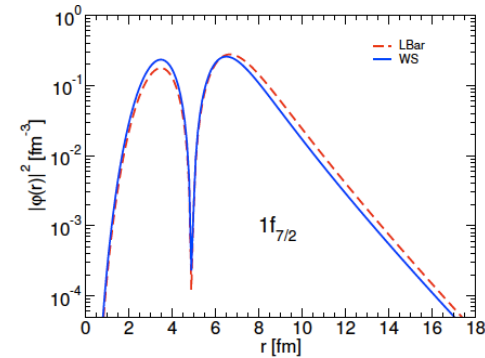


E	CH+ws	DOM
2	0.94	0.72
13	0.82	0.67
19.3	0.77	0.68
56	1.1	0.70

reactions and structure

$^{132}\text{Sn}(d,p)$

- Does it work when the potentials are extrapolated?

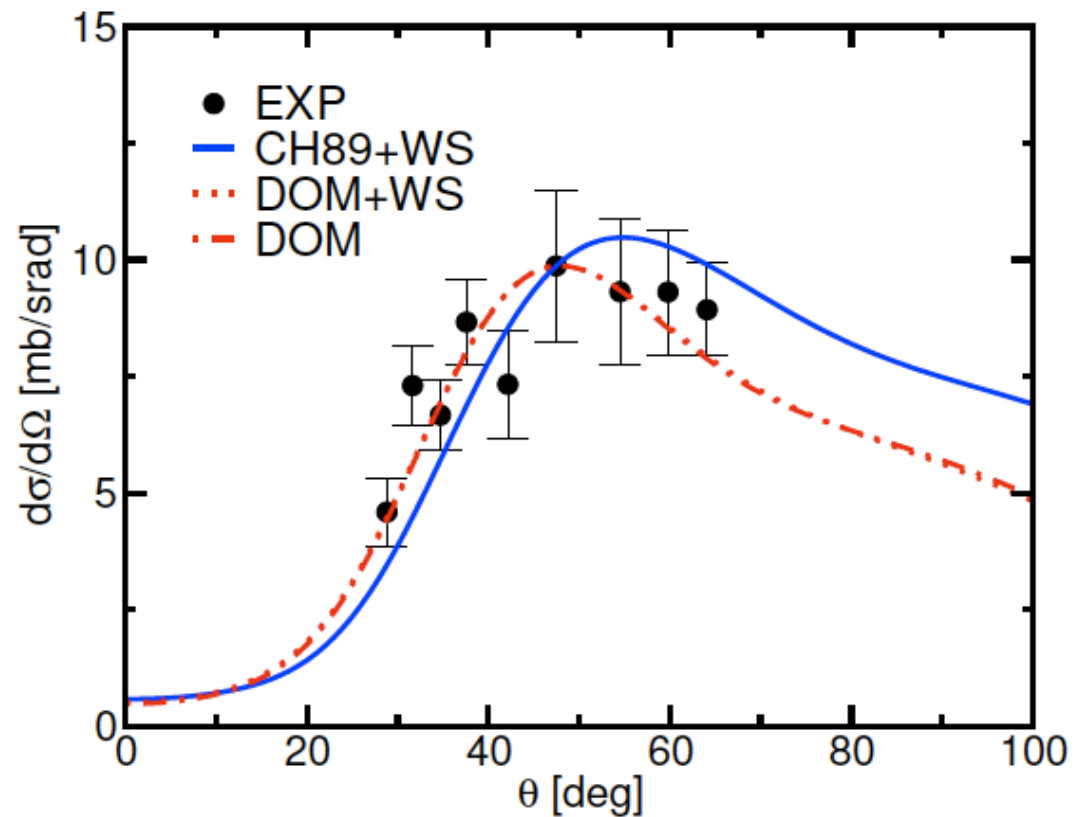


- Data: K.L. Jones et al., Nature 465, 454 (2010)

- $E_d = 9.46 \text{ MeV}$ $^{132}\text{Sn}(d,p)^{133}\text{Sn}$

- CH89+ws $\rightarrow S_{1f_{7/2}} = 1.1$

- DOM $\rightarrow S_{1f_{7/2}} = 0.72$



Propagator in principle generates

- Elastic scattering cross sections for p and n
- Including all polarization observables
- Total cross sections for n
- Reaction cross sections for p and n
- Overlap functions for adding p or n to bound states in Z+1 or N+1
- Plus normalization --> spectroscopic factor
- Overlap function for removing p or n with normalization
- Hole spectral function including high-momentum description
- One-body density matrix; occupation numbers; natural orbits
- Charge density
- Neutron distribution
- p and n distorted waves
- Contribution to the energy of the ground state from V_{NN}

DOM improvements

- Replace local energy-dependent HF potential by non-local (energy-independent potential) in order to calculate more properties below the Fermi energy like the charge density and spectral functions --> PRC82, 054306 (2010)

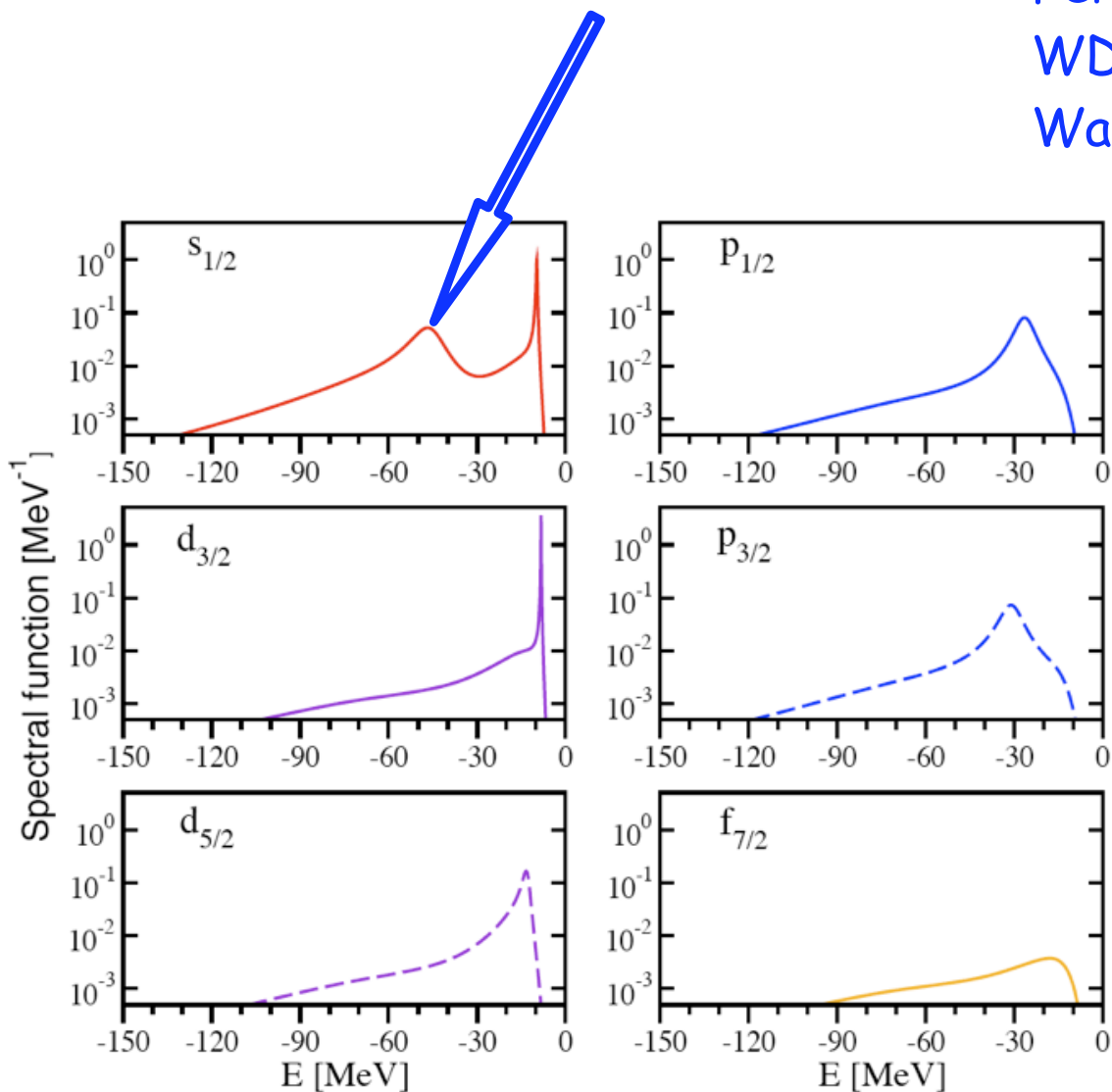
DOModel --> DOMethod-->DSelf-energyMethod

Below ϵ_F

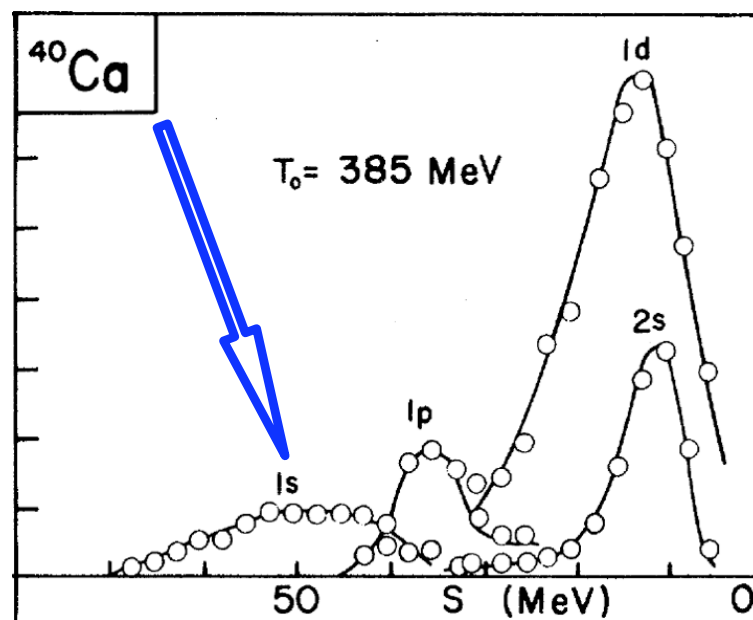
^{40}Ca spectral function

Recent theoretical development:
nonlocal "HF" self-energy --> below the
Fermi energy

WD, Van Neck, Charity, Sobotka,
Waldecker, PRC82, 054306 (2010)



Old (p,2p) data from Liverpool

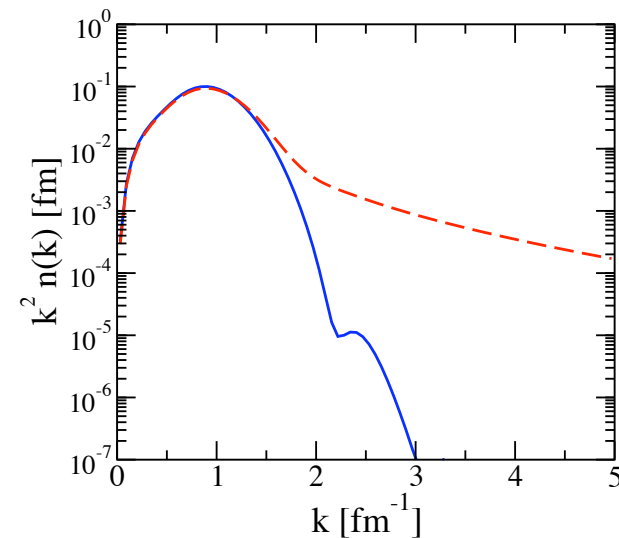
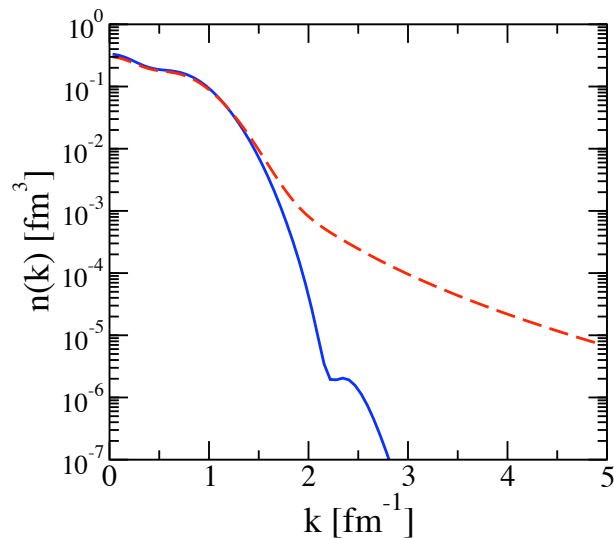
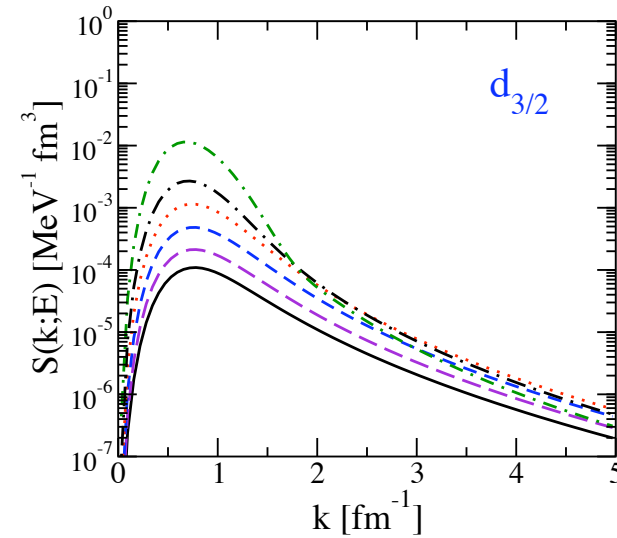
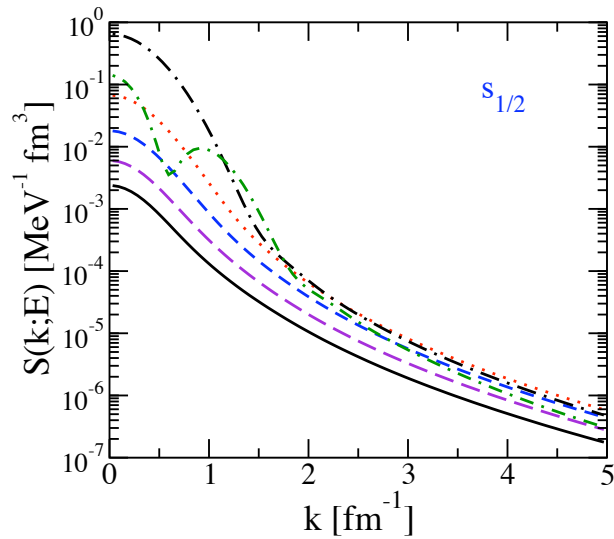


Understanding/Calculating Self-energy

Spectral functions and momentum distributions

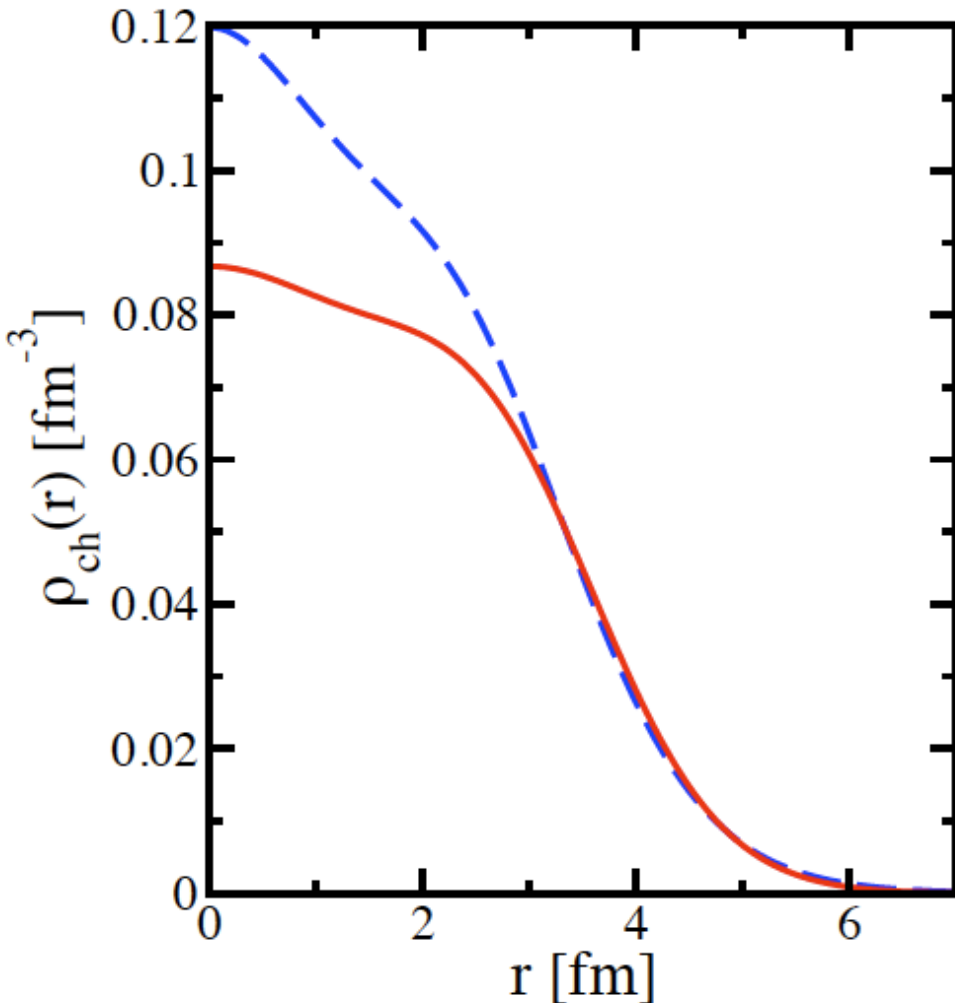
• ^{40}Ca

PRC 82, 054306 (2010)



Understanding/Calculating Self-energy

Charge density



Not a good reproduction of charge density even though mean square radius was fitted.

Related to local representation of the imaginary part of the self-energy --> independent of angular momentum --> must be abandoned to represent particle number correctly as well.

DOM extensions linked to ab initio FRPA

- Employ microscopic FRPA calculations of the nucleon self-energy to gain insight into future improvements of the DOM -->

S. J. Waldecker, C. Barbieri and W. H. Dickhoff

[Phys. Rev. C84, 034616 \(2011\), 1-11](#)

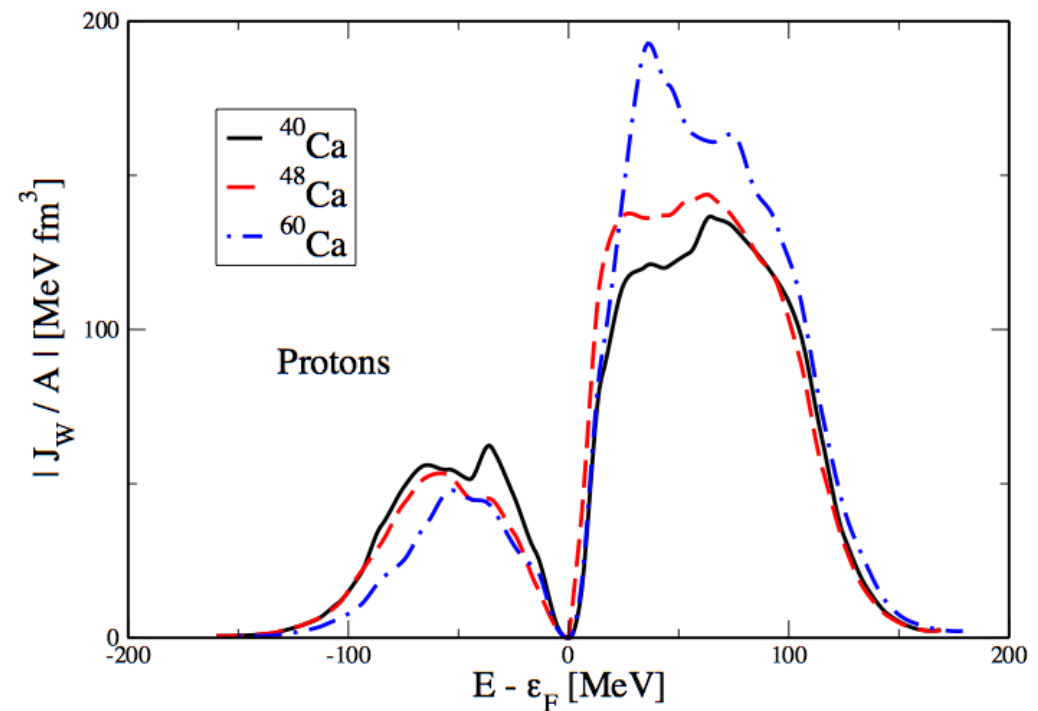
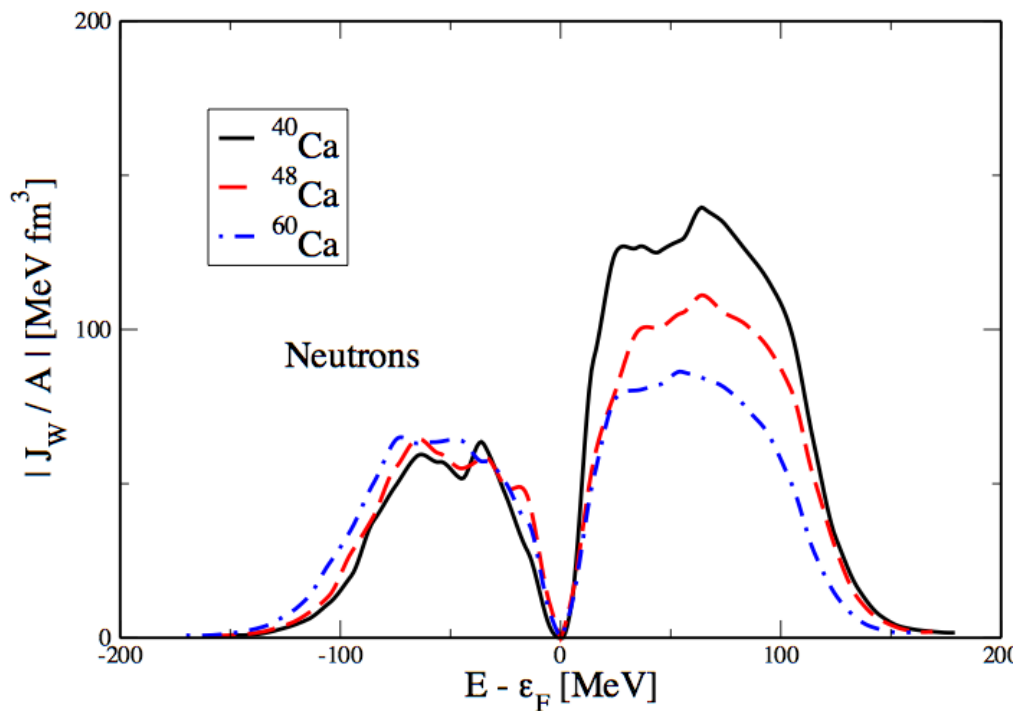
- FRPA = Faddeev RPA --> Barbieri for a recent application see e.g. PRL103,202502(2009)
- **Most important conclusions**
 - Ab initio self-energy has imaginary part with a substantial non-locality
 - Tensor force already operative for low-energy imaginary part
 - Absorption above and below Fermi energy not symmetric

Understanding/Calculating Self-energy

Volume integrals from microscopic FRPA relevant up to ~ 75 MeV

Volume integral for local imaginary potentials

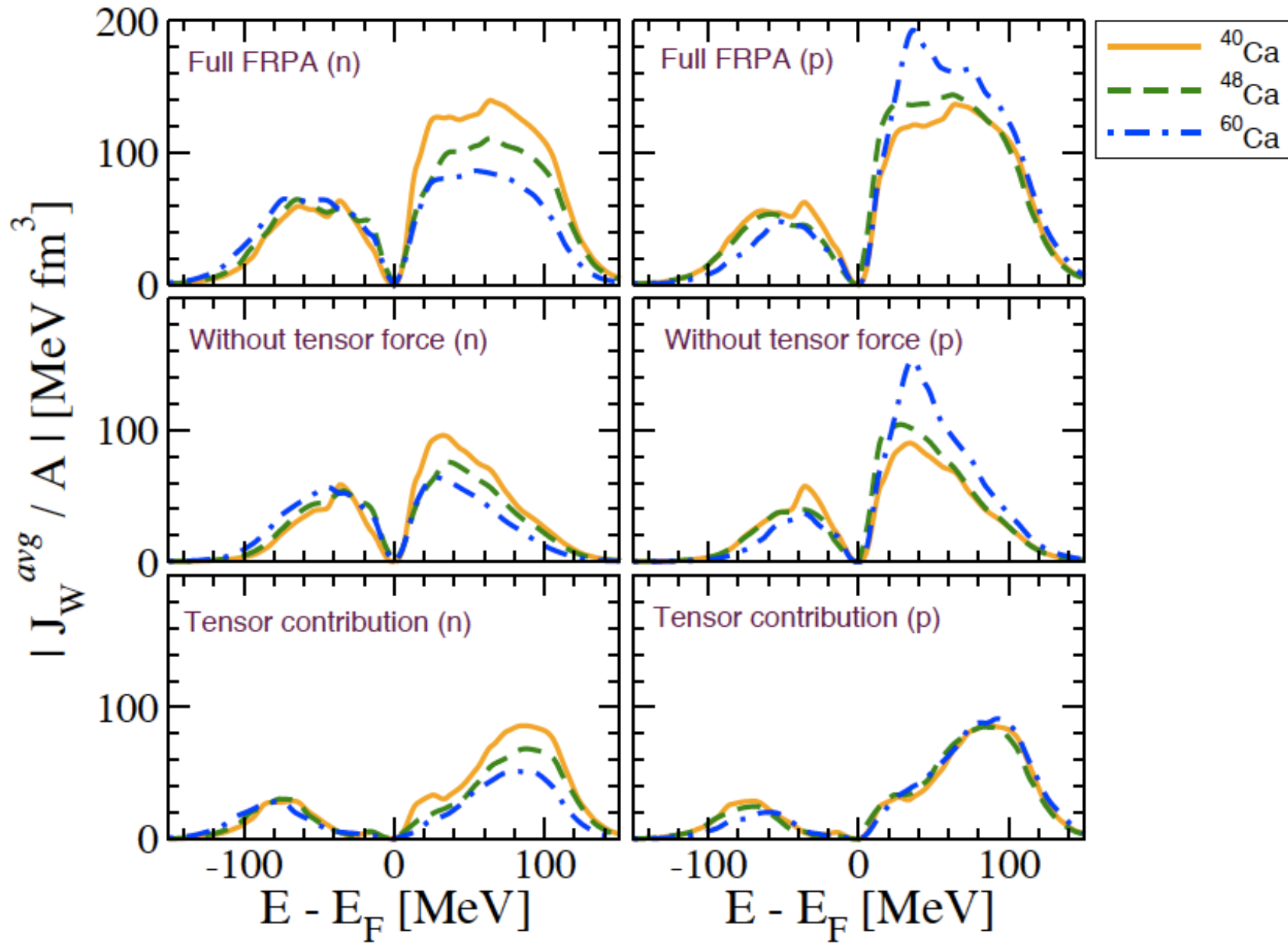
$$J_W(E) = 4\pi \int dr r^2 W(r, E)$$



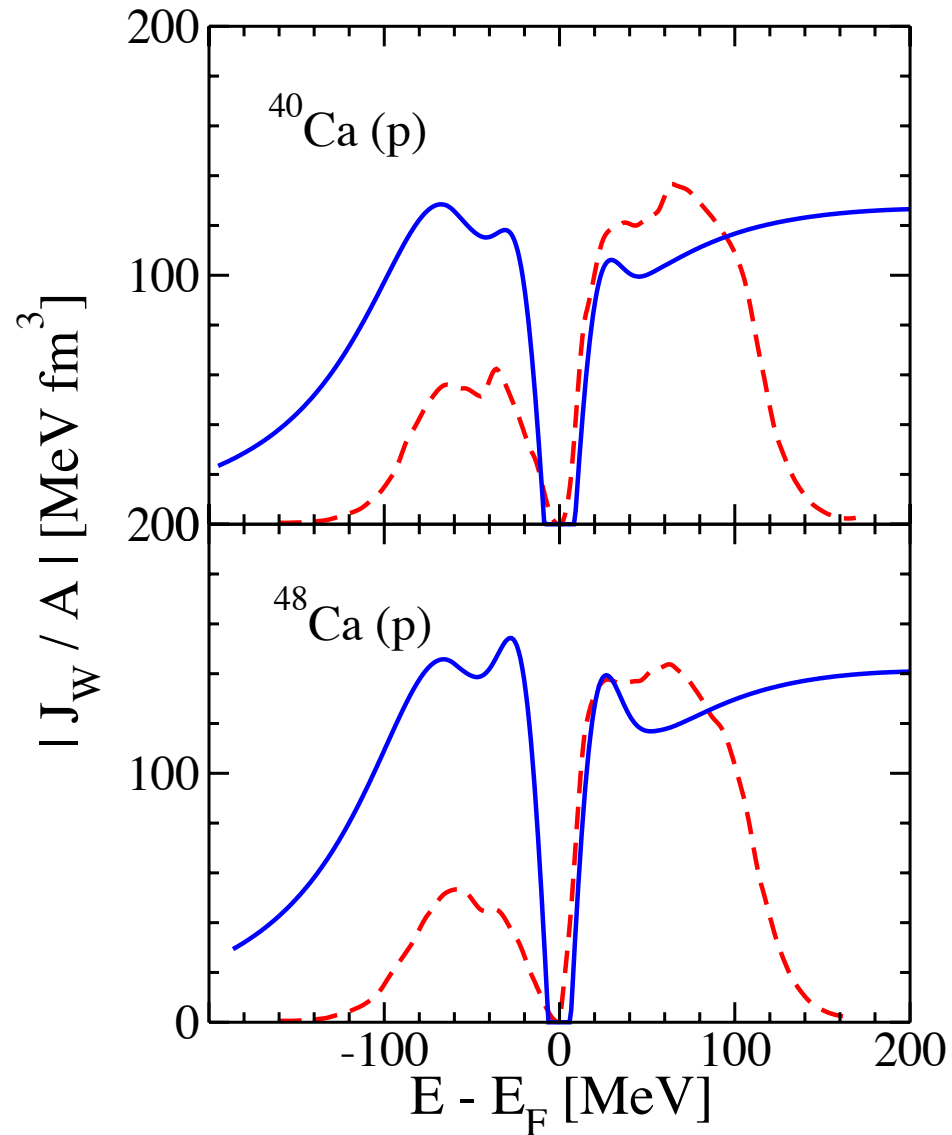
Microscopic potentials: nonlocal \rightarrow depend strongly on ℓ
Here averaged

Understanding/Calculating Self-energy

Tensor force



Comparison with DOM for $^{40,48}\text{Ca}$



DOM extensions linked to ab initio treatment of SRC

- Employ microscopic calculations of the nucleon self-energy to gain insight into future improvements of the DOM -->

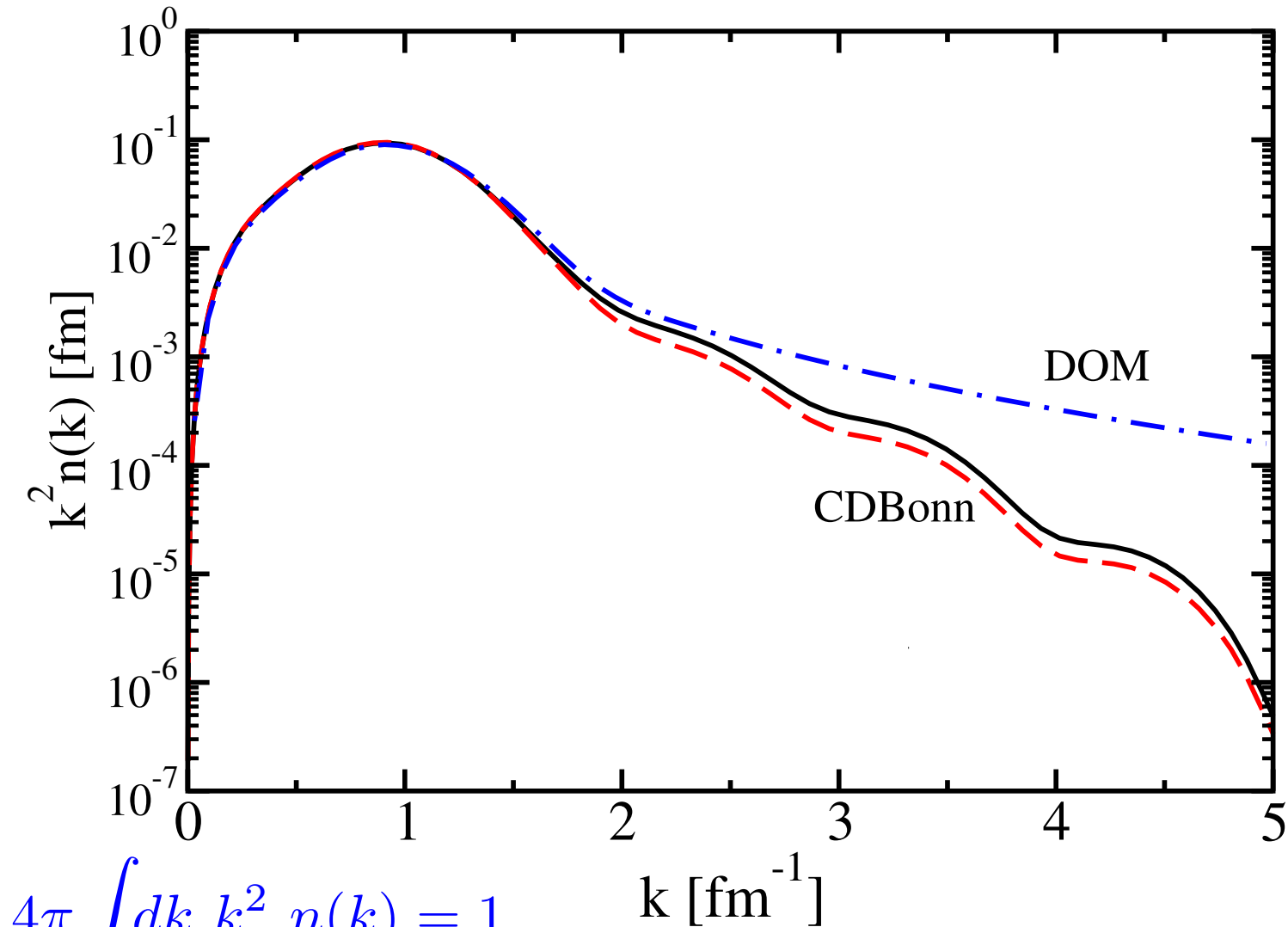
H. Dussan, S. J. Waldecker, W. H. Dickhoff, H. Mütter, and A. Polls

[Phys. Rev. C84, 044319 \(2011\), 1-16](#)

- CDBonn --> self-energy in momentum space for ^{40}Ca
- Most important conclusions
 - Volume absorption below the Fermi energy is also nonlocal
 - Reaction cross section comparable with DOM above ~ 80 MeV

Ab initio with CDBonn for ^{40}Ca

- Dussan et al. PRC84, 044319 (2011); spectral functions available



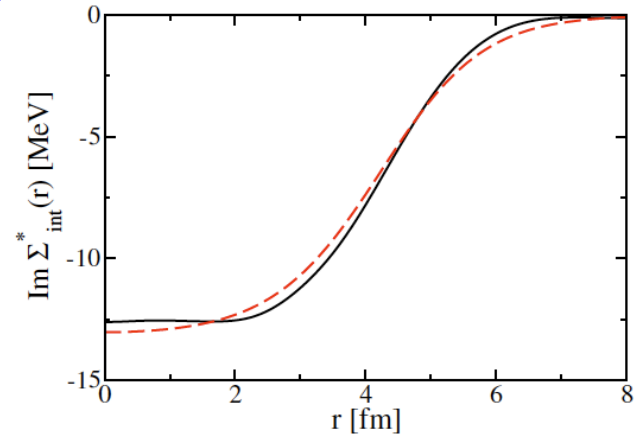
$$4\pi \int dk k^2 n(k) = 1$$

Non-locality of imaginary part

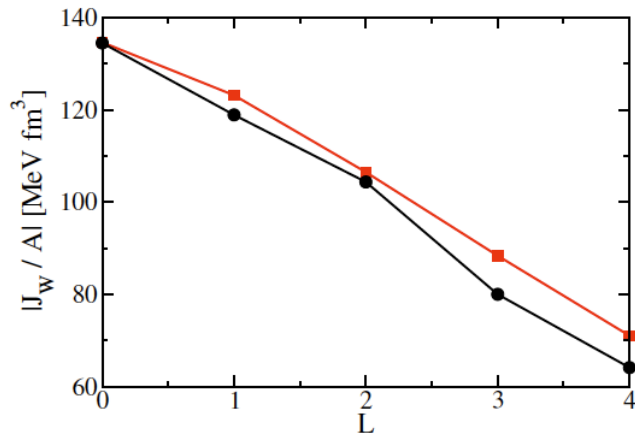
- Fit non-local imaginary part for $\ell=0$

$$W_{NL}(\mathbf{r}, \mathbf{r}') = W_0 \sqrt{f(r)} \sqrt{f(r')} H\left(\frac{r-r'}{\beta}\right)$$

- Integrate over one radial variable



- Predict volume integrals for higher ℓ



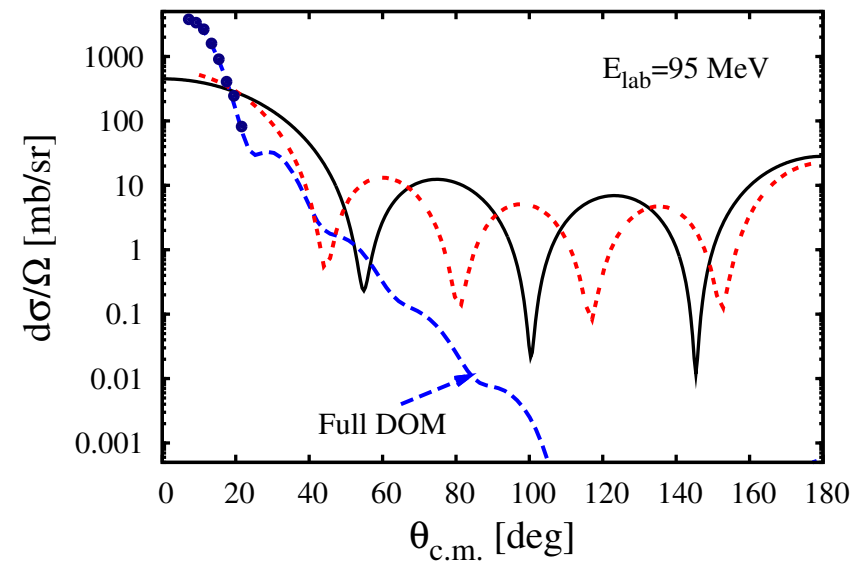
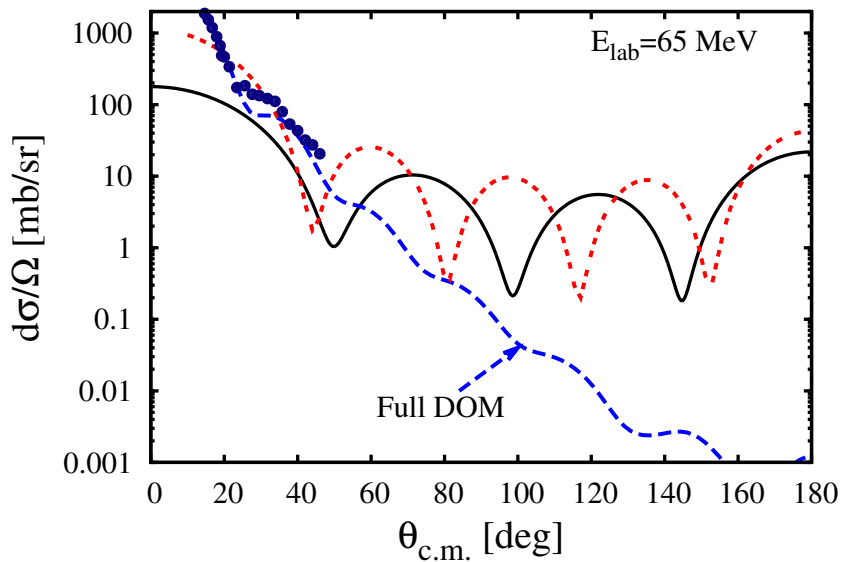
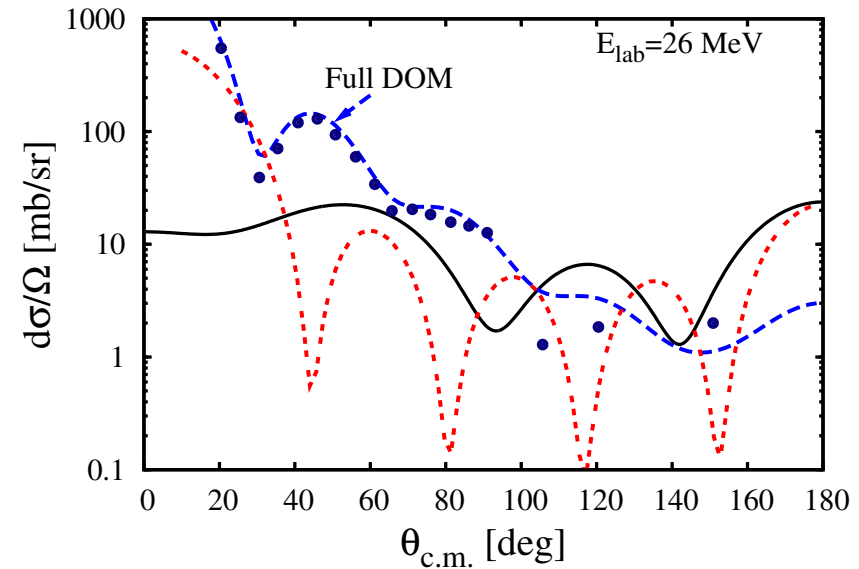
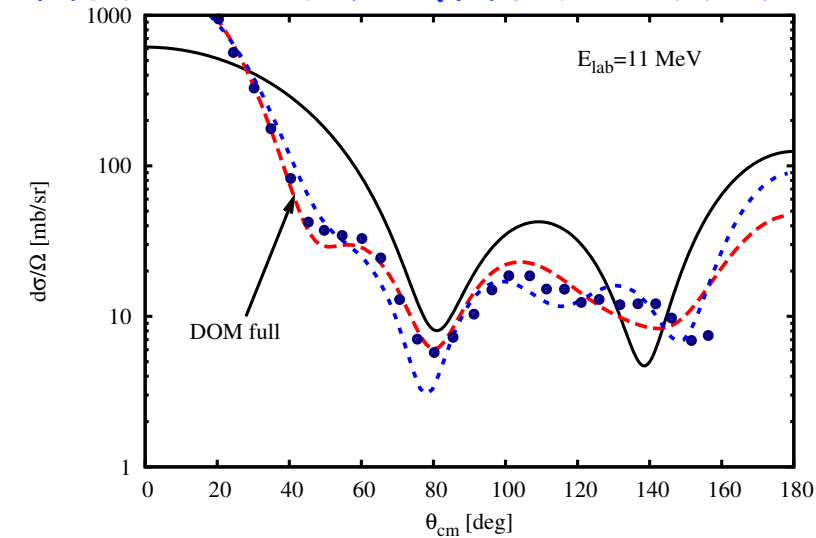
Parameters

Energy MeV	W_0	r_0	a_0	β	$ J_W/A $	$ J_W/A $ CDBonn
-76	36.30	0.90	0.90	1.33	193	193
49	6.51	1.25	0.91	1.43	73	73
65	13.21	1.27	0.70	1.29	135	135
81	23.90	1.22	0.67	1.21	215	215

Understanding/Calculating Self-energy

Ab initio description of elastic scattering

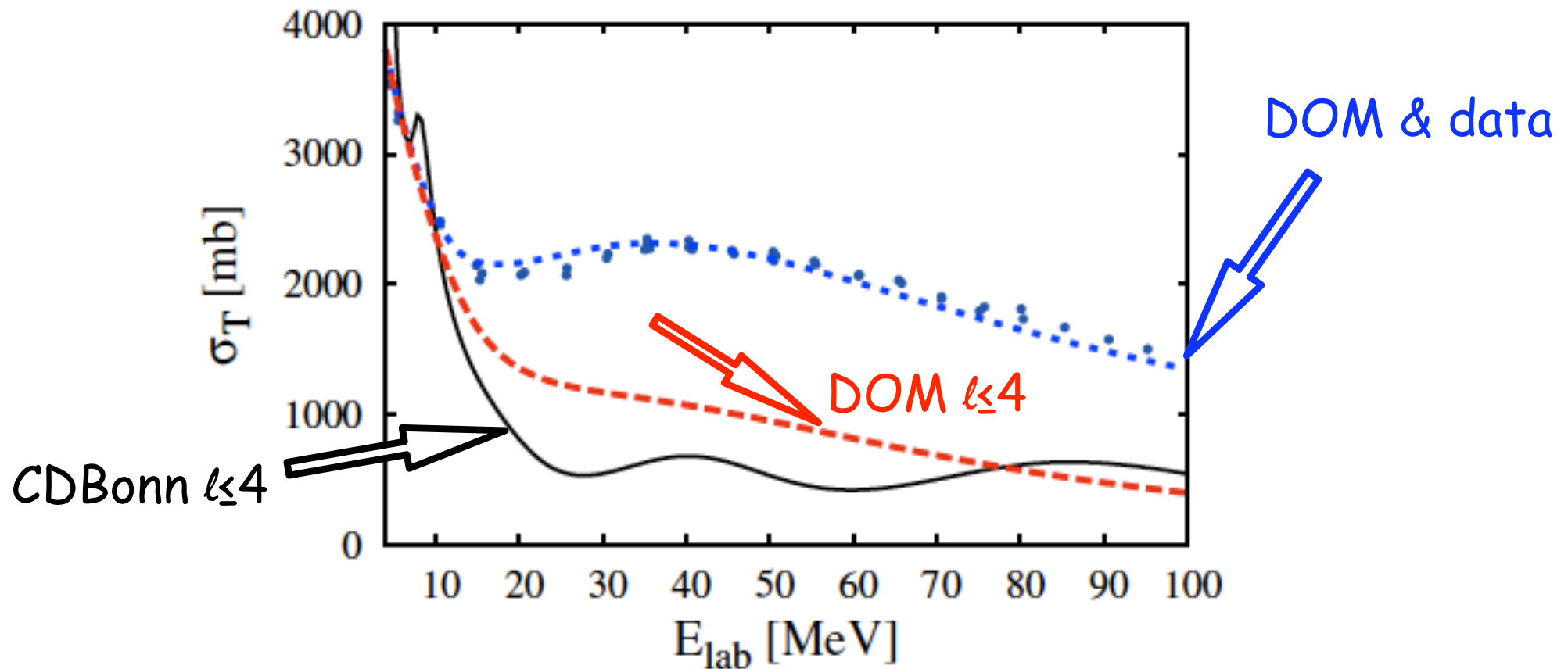
- Must be done much better



Understanding/Calculating Self-energy

Ab initio calculation of elastic scattering $n+^{40}\text{Ca}$

- ONLY treatment of short-range and tensor correlations

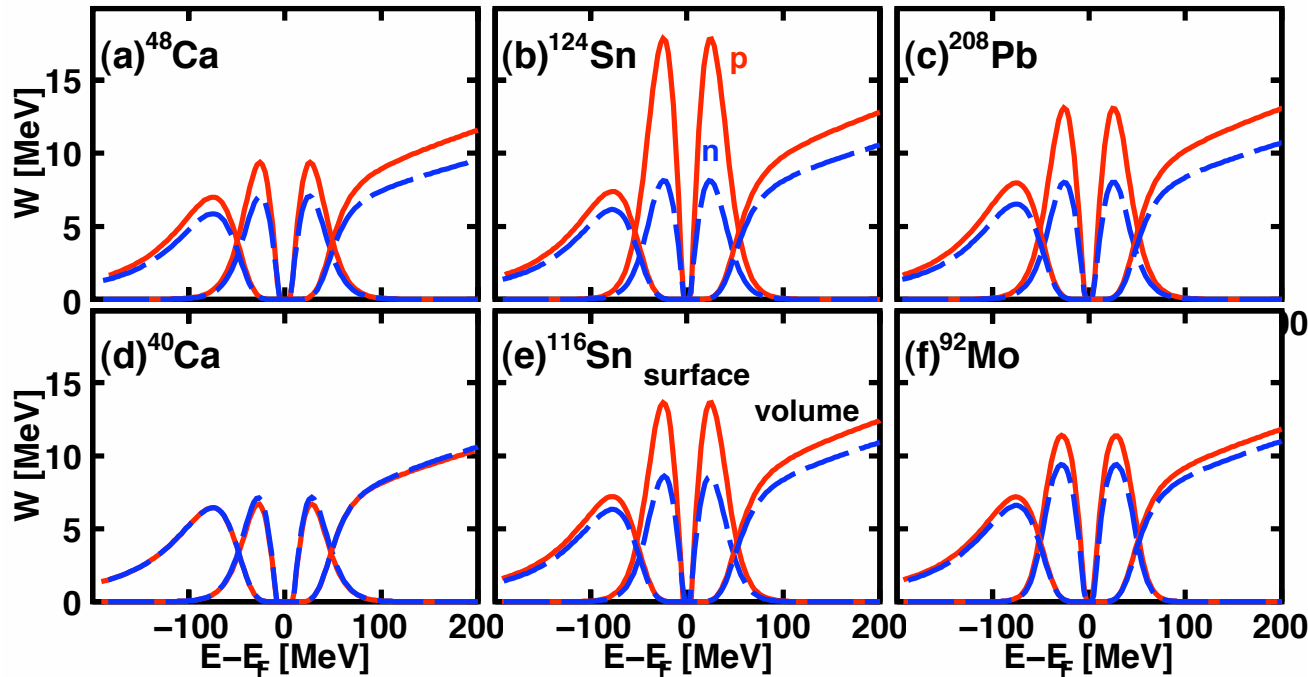


Understanding/Calculating Self-energy

DOM predictions

- Use non-local "HF" potential and dispersive DOM potential to extrapolate to unstable Sn isotopes and predict (e.g.) properties of the last proton (based on the analysis of elastic scattering data on **STABLE** Sn nuclei)

Asymmetry dependence of imaginary potentials

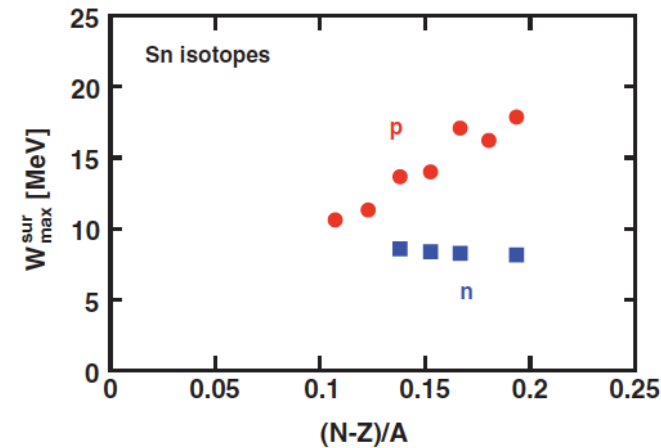


- Volume \rightarrow small asymmetry dependence determined

in ^{208}Pb

$$W_{\text{volume}} = W_{\text{volume}}^0 \pm \frac{N-Z}{A} W_{\text{volume}}^1$$

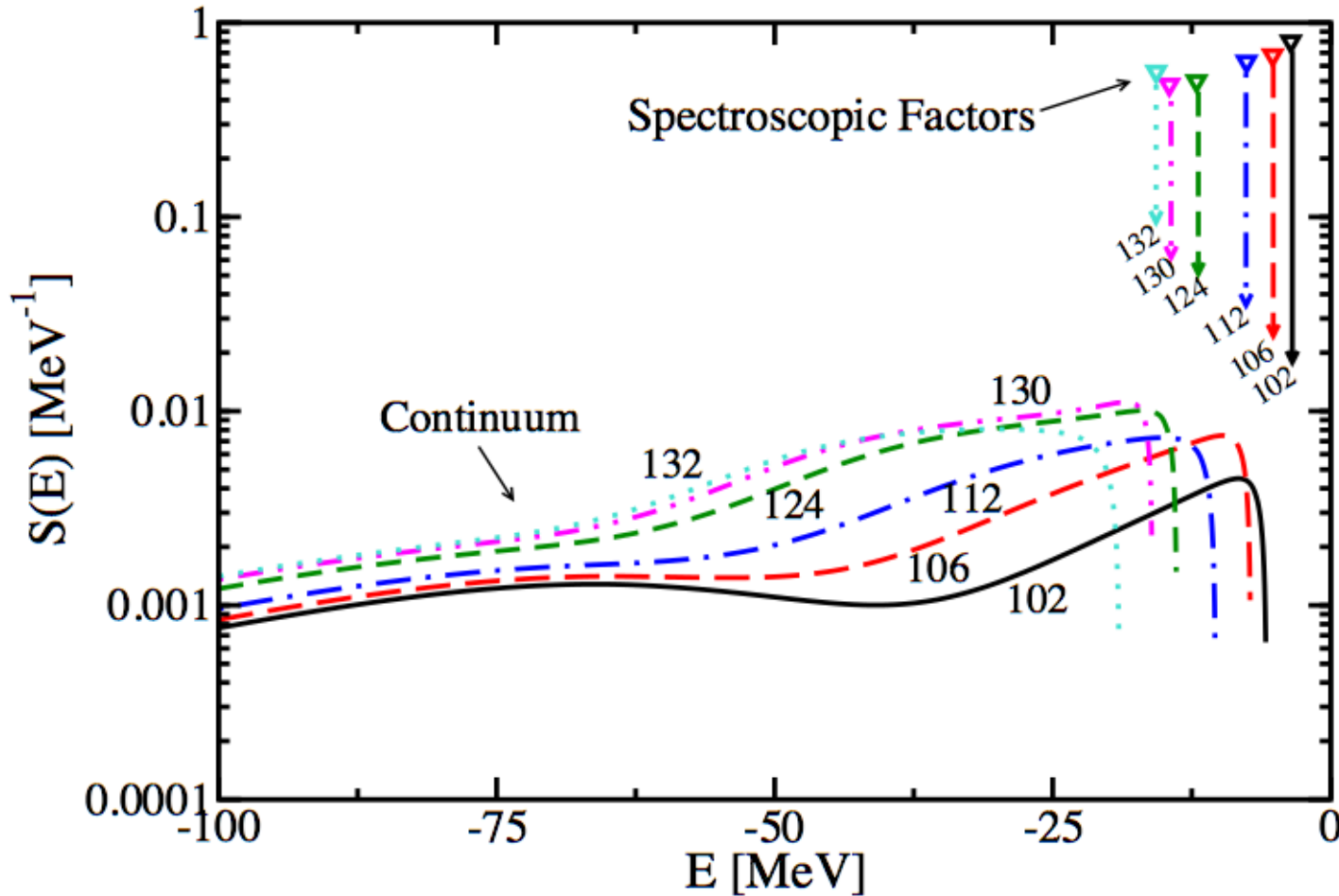
- Neutron surface \rightarrow no strong dependencies on A or $(N-Z)/A$
- Proton surface absorption \rightarrow increases with increasing neutron number



reactions and structure

Last proton in Sn nuclei ($g_{9/2}$)

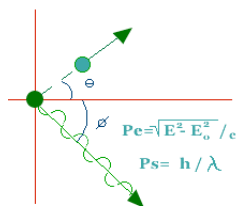
Spectral function for different Sn isotopes



Sn	S	n
102	0.80	0.91
106	0.68	0.85
112	0.63	0.83
124	0.50	0.78
130	0.48	0.78
132	0.56	0.81

People involved

 Washington
University in St. Louis



Wim Dickhoff

Bob Charity

Lee Sobotka

Helber Dussan

Seth Waldecker

Hossein Mahzoon

Dong Ding

Carlo Barbieri, Surrey

Arnau Rios, Surrey

Arturo Polls, Barcelona

Dimitri Van Neck, Ghent

Herbert Müther, Tübingen



Universitat de Barcelona



EBERHARD KARLS
UNIVERSITÄT
TÜBINGEN



N.B. Nguyen & F. Nuñez

Dispersive Optical Model

- Claude Mahaux 1980s
 - connect traditional optical potential to bound-state potential
 - crucial idea: use the dispersion relation for the nucleon self-energy
 - smart implementation: use it in its subtracted form
 - applied successfully to ^{40}Ca and ^{208}Pb in a limited energy window
 - employed traditional volume and surface absorption potentials and a local energy-dependent Hartree-Fock-like potential
 - Reviewed in *Adv. Nucl. Phys.* **20**, 1 (1991)
- Radiochemistry group at Washington University in St. Louis: Charity and Sobotka propose to use it for a sequence of Ca isotopes → data-driven extrapolations to the drip line
 - First results 2006 PRL
 - Subsequently → attention to data below the Fermi energy related to ground-state properties → Dispersive Self-energy Method (**DSM**)

Optical potential \leftrightarrow nucleon self-energy

- e.g. Bell and Squires \rightarrow elastic T-matrix = reducible self-energy
- Mahaux and Sartor *Adv. Nucl. Phys.* **20**, 1 (1991)
 - relate dynamic (energy-dependent) real part to imaginary part
 - employ subtracted dispersion relation

General dispersion relation for self-energy:

$$\text{Re } \Sigma(E) = \Sigma^{HF} - \frac{1}{\pi} \mathcal{P} \int_{E_T^+}^{\infty} dE' \frac{\text{Im } \Sigma(E')}{E - E'} + \frac{1}{\pi} \mathcal{P} \int_{-\infty}^{E_T^-} dE' \frac{\text{Im } \Sigma(E')}{E - E'}$$

Calculated at the Fermi energy $\varepsilon_F = \frac{1}{2} \{ (E_0^{A+1} - E_0^A) + (E_0^A - E_0^{A-1}) \}$

$$\text{Re } \Sigma(\varepsilon_F) = \Sigma^{HF} - \frac{1}{\pi} \mathcal{P} \int_{E_T^+}^{\infty} dE' \frac{\text{Im } \Sigma(E')}{\varepsilon_F - E'} + \frac{1}{\pi} \mathcal{P} \int_{-\infty}^{E_T^-} dE' \frac{\text{Im } \Sigma(E')}{\varepsilon_F - E'}$$

Subtract

$$\text{Re } \Sigma(E) = \text{Re } \widetilde{\Sigma}^{HF}(\varepsilon_F)$$

$$- \frac{1}{\pi} (\varepsilon_F - E) \mathcal{P} \int_{E_T^+}^{\infty} dE' \frac{\text{Im } \Sigma(E')}{(E - E')(\varepsilon_F - E')} + \frac{1}{\pi} (\varepsilon_F - E) \mathcal{P} \int_{-\infty}^{E_T^-} dE' \frac{\text{Im } \Sigma(E')}{(E - E')(\varepsilon_F - E')}$$

Nonlocal DOM implementation PRL112,162503(2014)

- Particle number --> **nonlocal** imaginary part
- Microscopic FRPA & SRC --> different nonlocal properties above and below the Fermi energy
- Include charge density in fit
- Describe high-momentum nucleons <--> (e,e'p) data from JLab

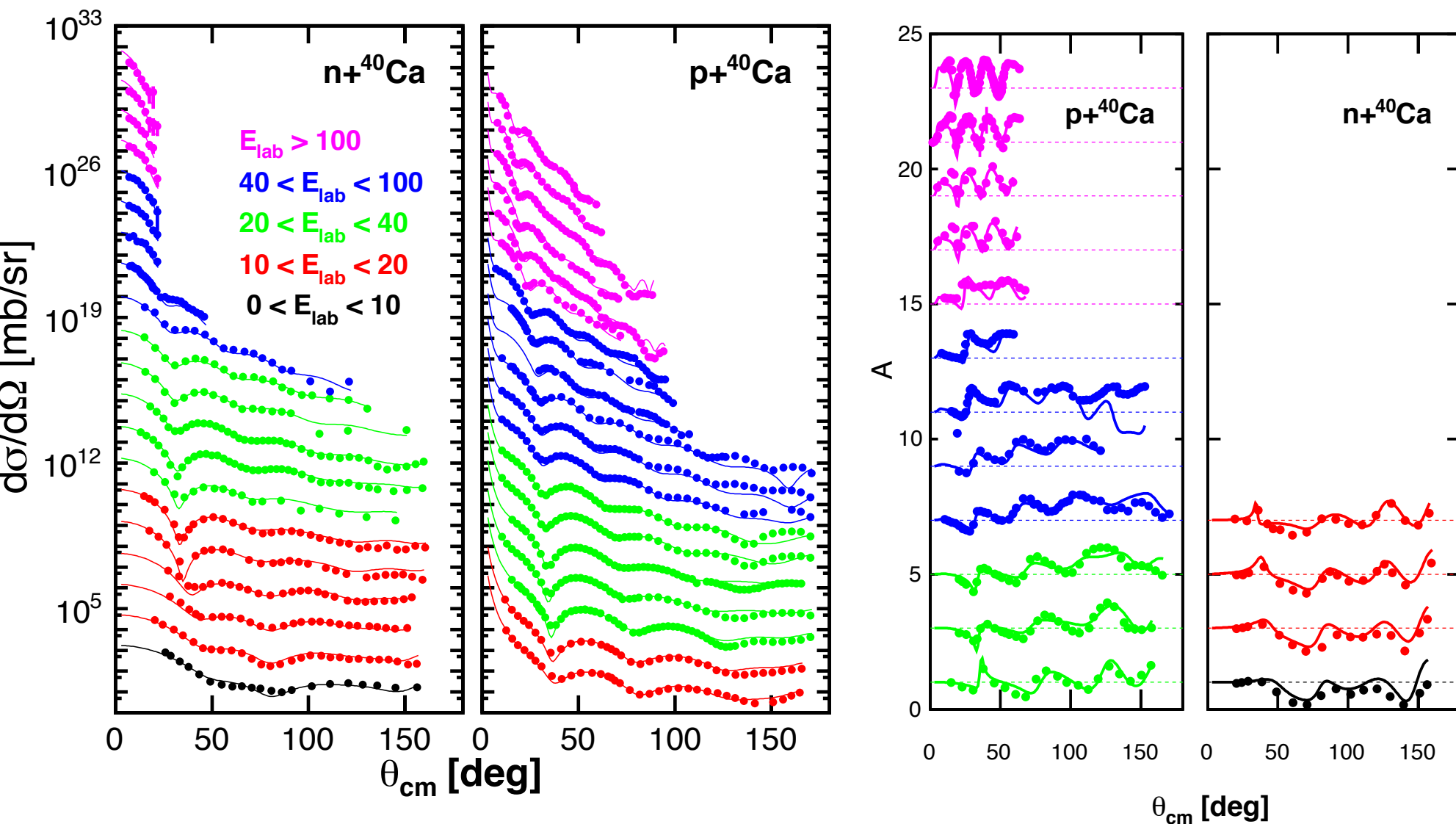
Implications

- Changes the description of hadronic reactions because interior nucleon wave functions depend on non-locality
- Consistency test of the interpretation of (e,e'p) possible
- Independent "experimental" statement on size of three-body contribution to the energy of the ground state--> two-body only:

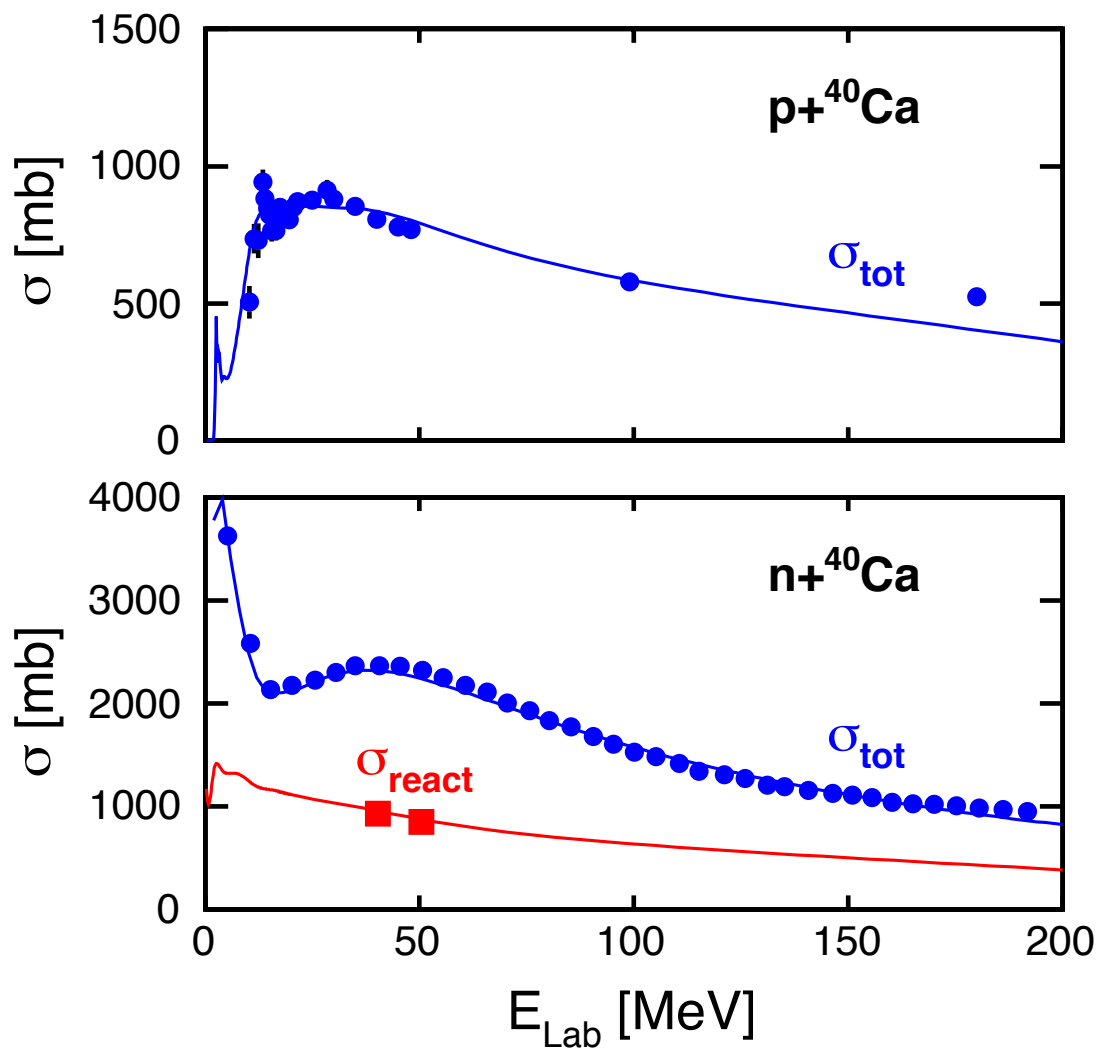
$$E/A = \frac{1}{2A} \sum_{\ell_j} (2j+1) \int_0^{\infty} dk k^2 \frac{k^2}{2m} n_{\ell_j}(k) + \frac{1}{2A} \sum_{\ell_j} (2j+1) \int_0^{\infty} dk k^2 \int_{-\infty}^{\epsilon_F} dE ES_{\ell_j}(k; E)$$

reactions and structure

Differential cross sections and analyzing powers



Reaction (p&n) and total (n) cross sections



Below ϵ_F

^{40}Ca spectral function

Nonlocal imaginary self-energy:

proton number $\rightarrow 19.88$

neutron number $\rightarrow 19.79$

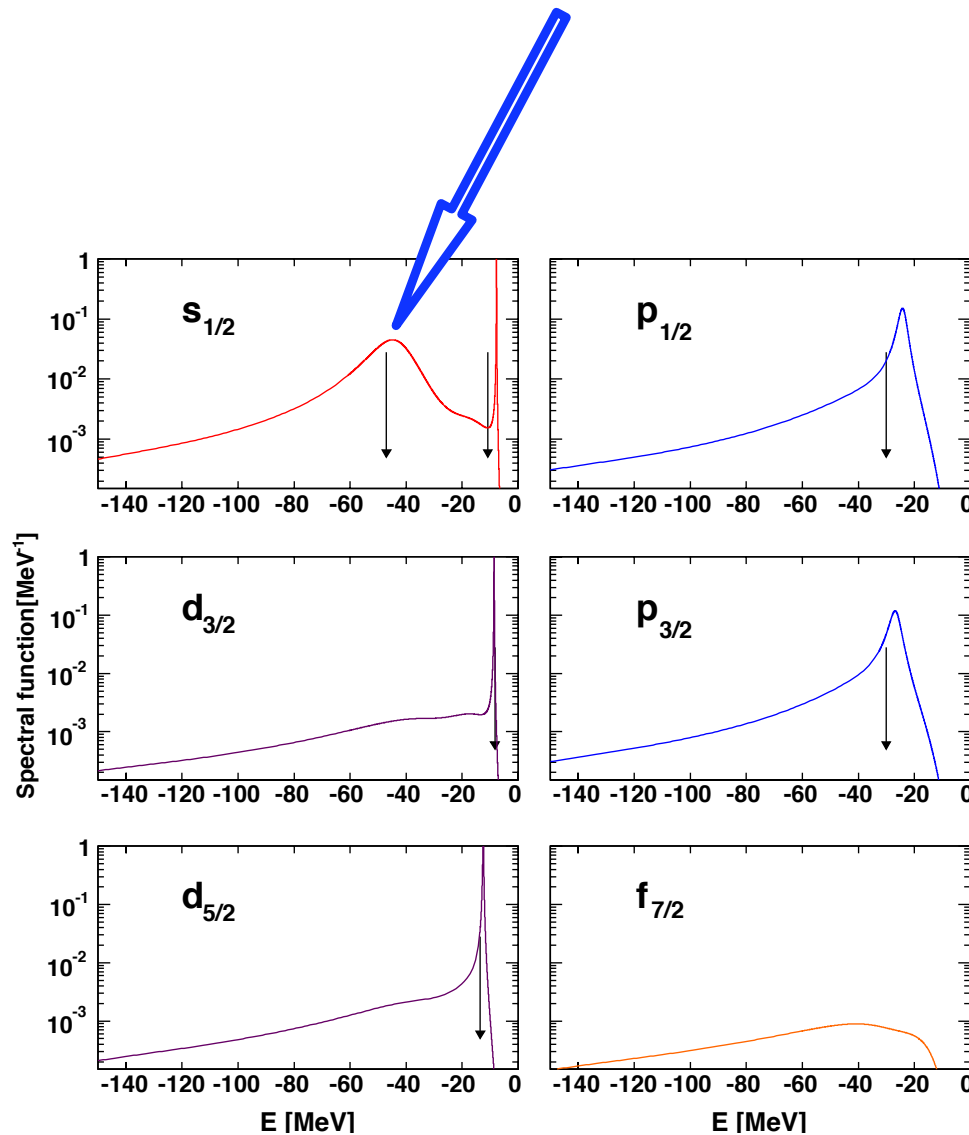
$$l \leq 5$$

$S_{0d_{3/2}} = 0.76$

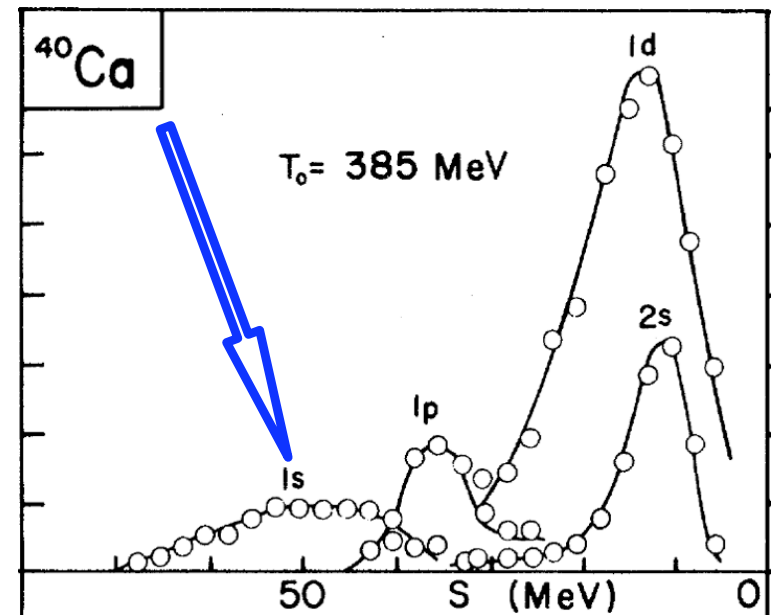
$S_{1s_{1/2}} = 0.78$

Not part of fit!!

0.15 larger than NIKHEF analysis!

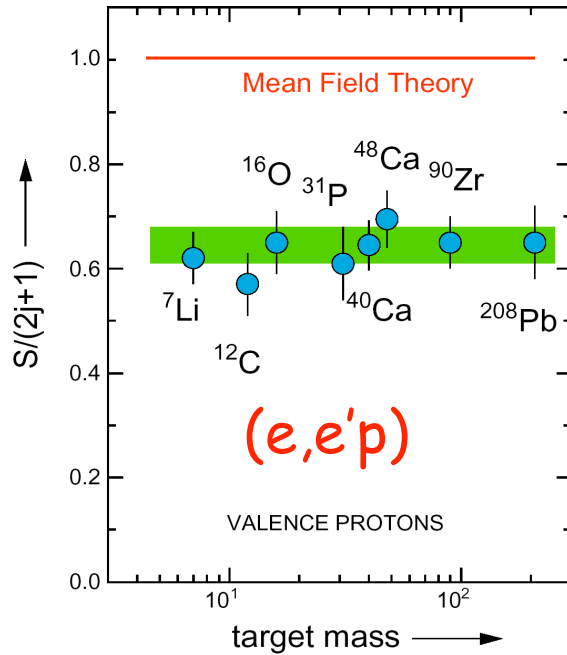


Old (p,2p) data from Liverpool
or (e,e'p) from Saclay



Linking nuclear reactions and nuclear structure → DOM

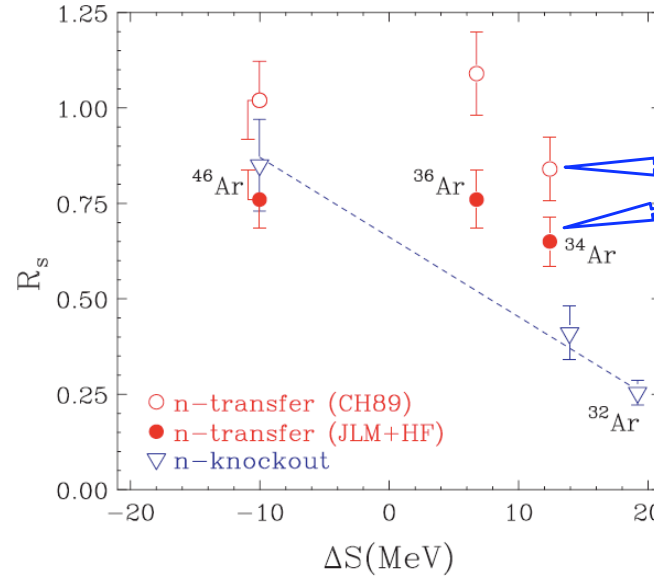
Correlations from nuclear reactions



In $(e,e'p)$ proton still has to get out of the nucleus → optical potential

Nucl. Phys. A553,297c (1993)

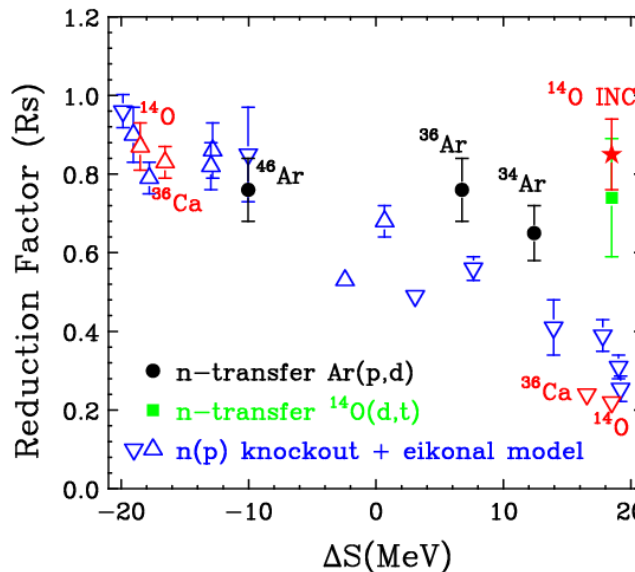
Consistency study in progress



Different optical potentials → different reduction factors for transfer reactions
Spectroscopic factors > 1 ???

PRL 93, 042501 (2004) HI

PRL 104, 112701 (2010) Transfer

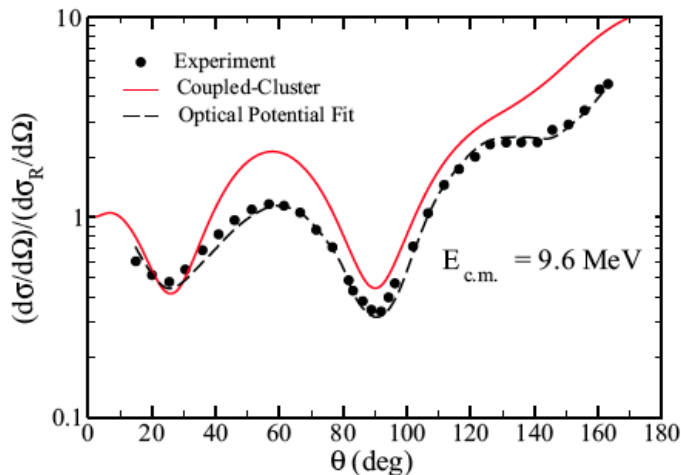


Recent summary → Jenny Lee

Different reactions different results???

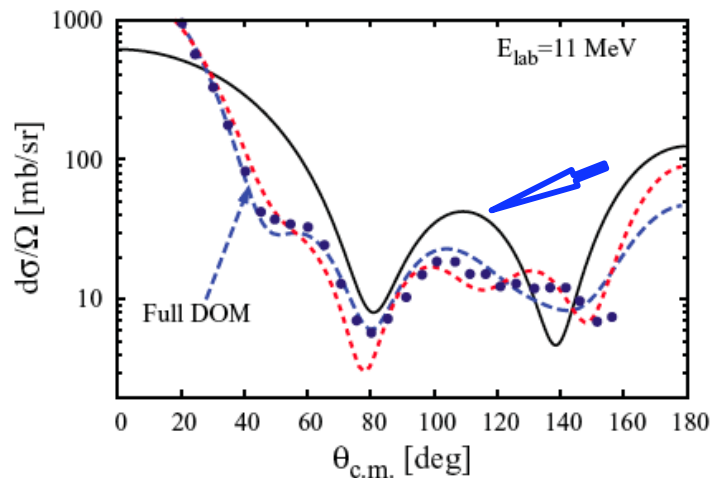
Linking nuclear reactions and nuclear structure

- Extracting information on correlations beyond the independent particle model requires **optical potentials** in (e,e'p), (d,p),(p,d),(p,pN), etc.
- Quality of **ab initio** to describe elastic scattering or optical potentials should be improved substantially and **urgently**



^{40}Ca

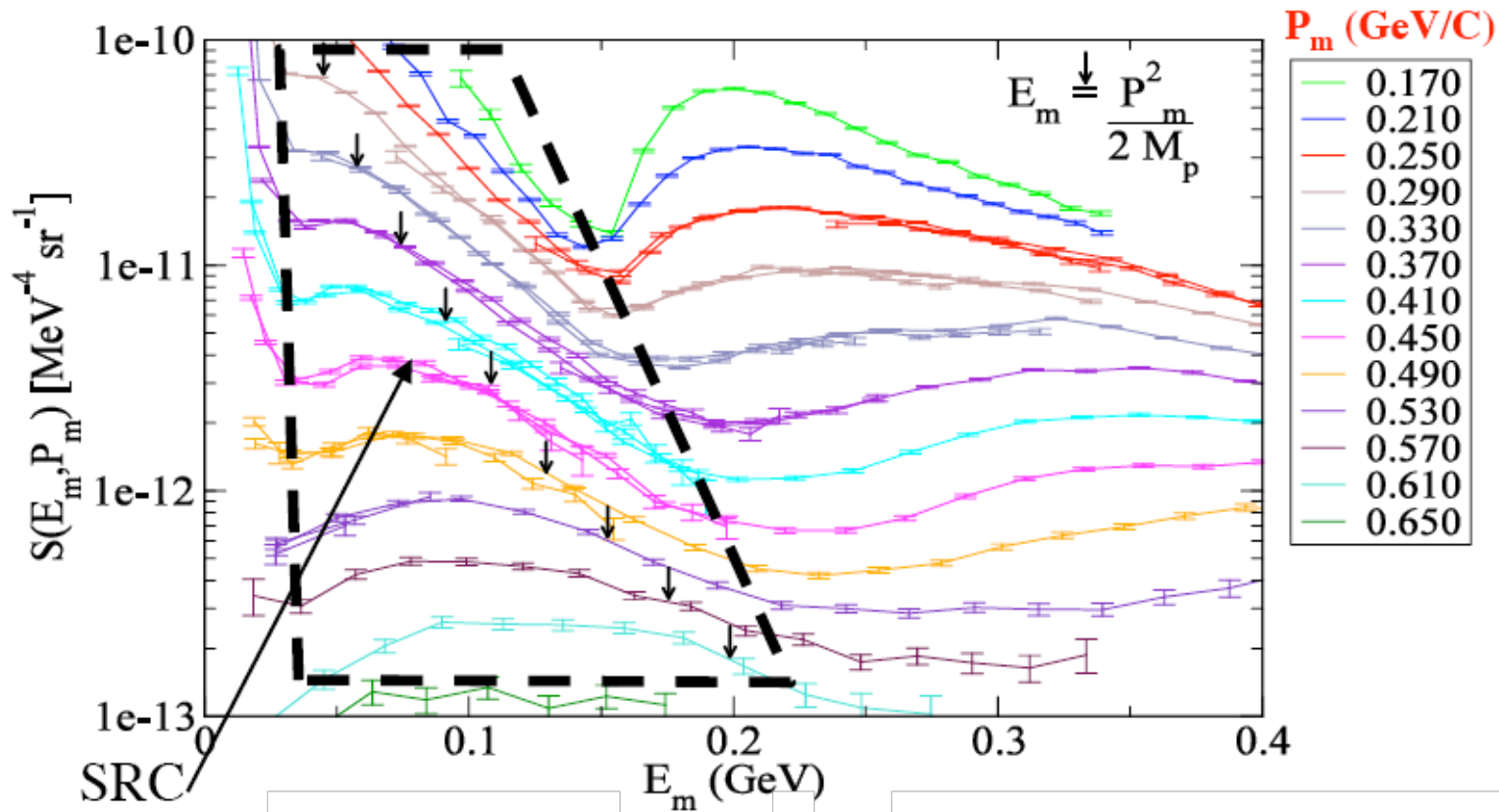
Coupled cluster calculation using overlap functions
PRC86,021602(R)(2012)
Probably limited to low energy



Green's function result \rightarrow optical potential with emphasis on SRC only
PRC84,044319(2011)

High-momentum protons have been seen in nuclei!

Jlab E97-006 Phys. Rev. Lett. 93, 182501 (2004) D. Rohe et al.



^{12}C

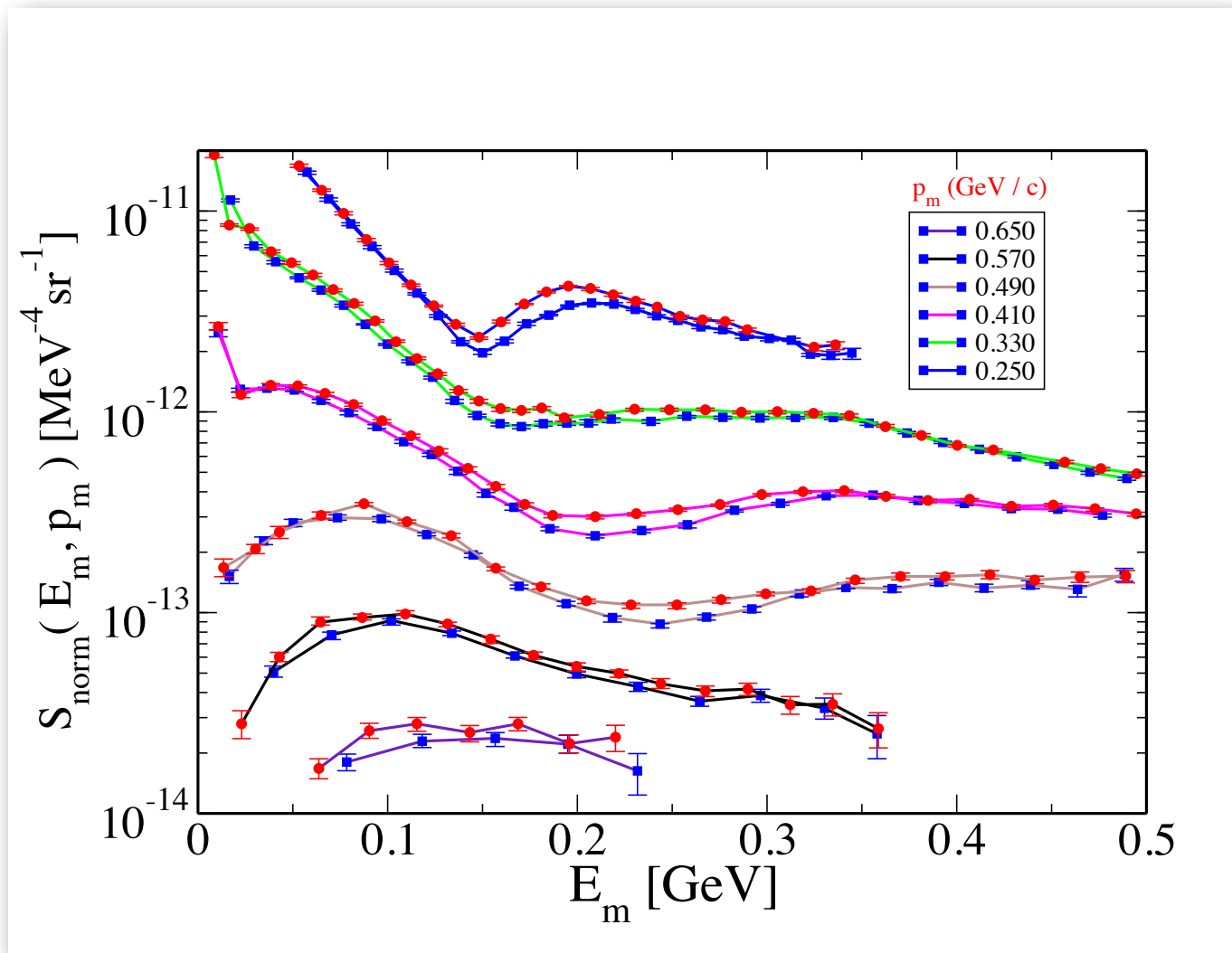
- Location of high-momentum components
- Integrated strength agrees with theoretical prediction Phys. Rev. C49, R17 (1994)

$\Rightarrow \sim 0.6$ protons for $^{12}\text{C} \Rightarrow \sim 10\%$

reactions and structure

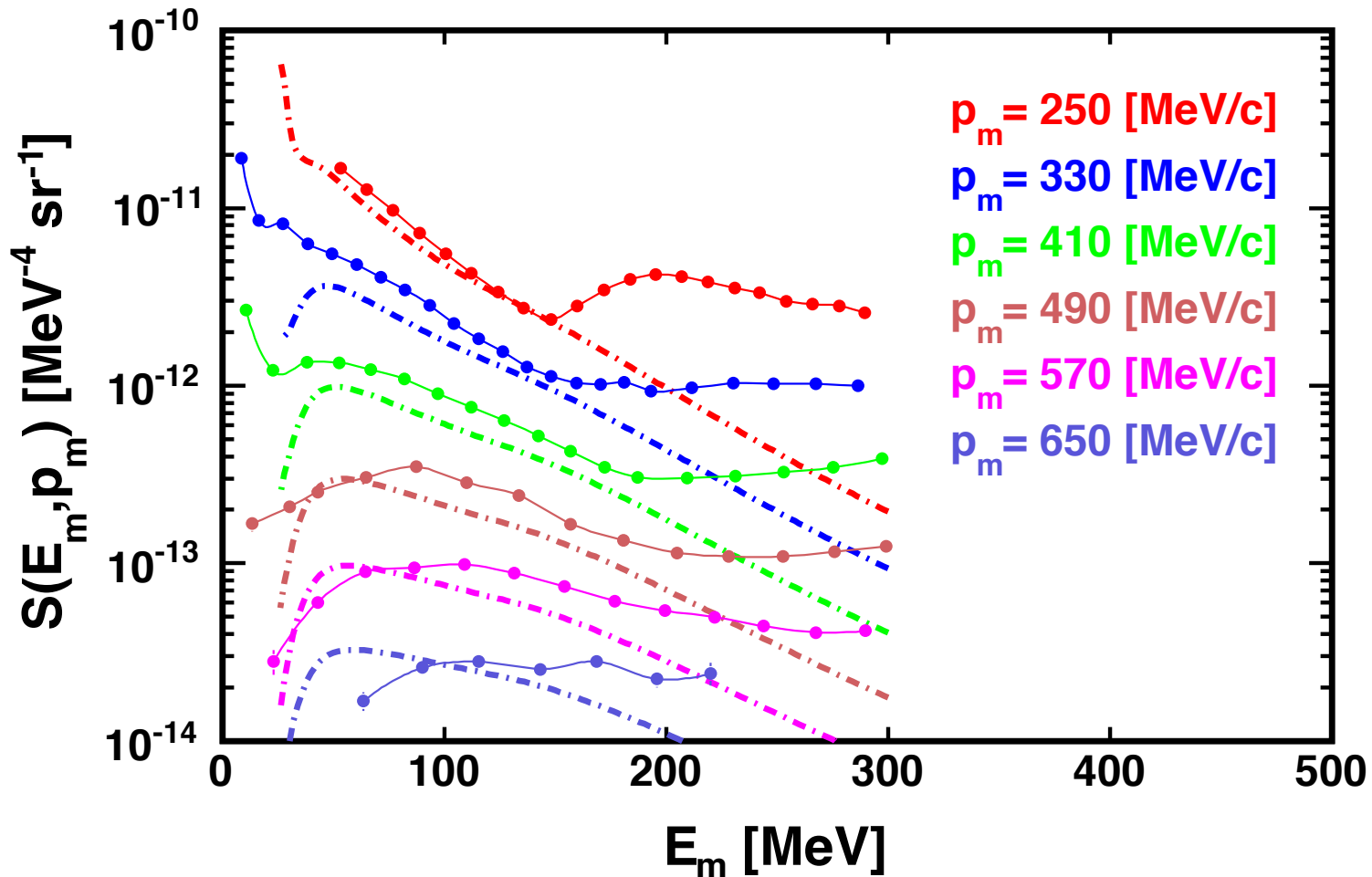
High-momentum components

Rohe, Sick et al. JLab data for Al and Fe ($e, e'p$)
per proton



Jefferson Lab data per proton

- Pion/isobar contributions cannot be described
- Rescattering contributes some cross section (Barbieri, Lapikas)

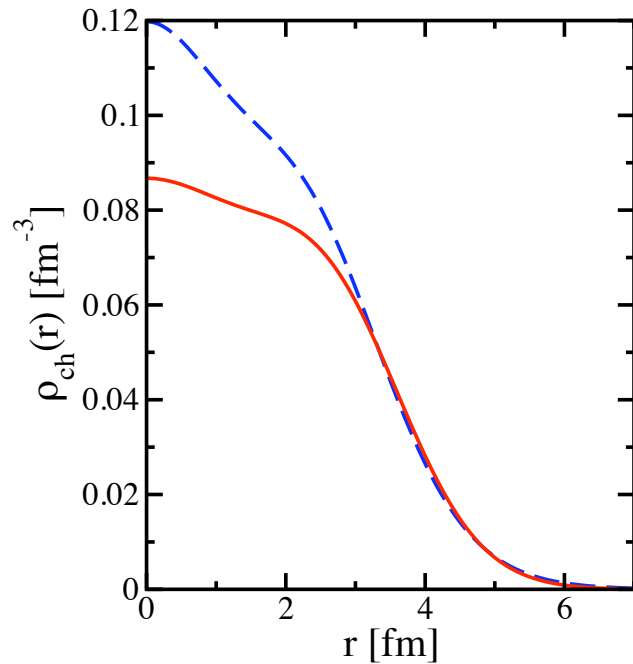


Critical experimental data

Local version

radius correct...

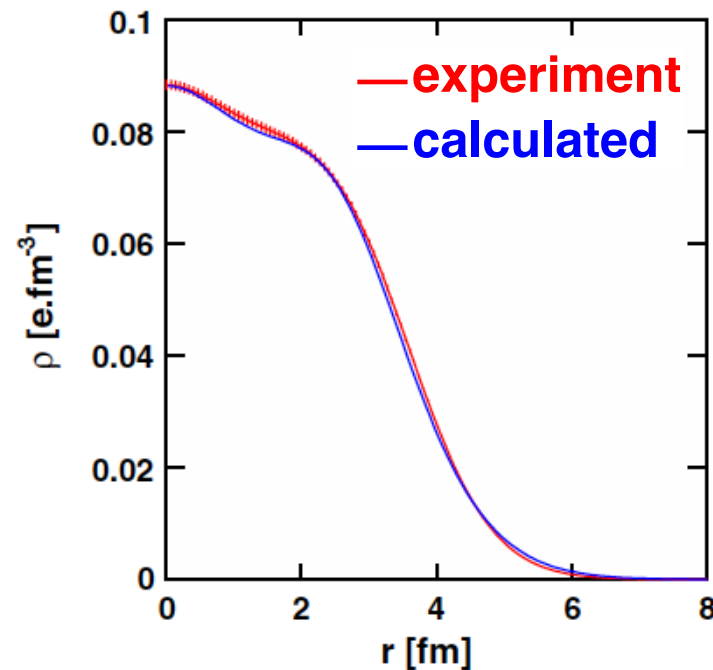
PRC82,054306(2010)



Charge density ^{40}Ca

Non-locality essential

PRL112,162503(2014)



High-momentum nucleons \rightarrow JLab can also be described \rightarrow E/A

Historical perspective...

- The following authors identify the single-particle propagator (or self-energy) as central quantities in many-body systems

Abrikosov, Gorkov, Dzyaloshinski

(Methods of Quantum Field Theory in Statistical Physics, 1963 Dover Revised edition 1975),

Pines

(The Many-body Problem, 1961 Addison Wesley reissued 1997),

Nozieres

(Theory of Interacting Fermi Systems, 1964 Addison-Wesley reissued 1997),

Thouless

(The Quantum Mechanics of Many-body Systems, 1972 Dover reissue of second edition, 2014),

Anderson

(Concepts in Solids, Benjamin 1963; World Scientific reissued 1998),

Schrieffer

(Theory of Superconductivity, 1964 Benjamin revised 1983),

Migdal

(Theory of Finite Fermi Systems and Applications to Atomic Nuclei (Interscience, 1967),

Fetter and Walecka

(Quantum Theory of Many-particle Systems, 1971 Dover reissued 2003)

- but apart from qualitative features, they don't answer what it looks like for a real system like a nucleus!

Energy of the ground state

- Energy sum rule (Migdal, Galitski & Koltun)

$$E/A = \frac{1}{2A} \sum_{\ell_j} (2j+1) \int_0^\infty dk k^2 \frac{k^2}{2m} n_{\ell_j}(k) + \frac{1}{2A} \sum_{\ell_j} (2j+1) \int_0^\infty dk k^2 \int_{-\infty}^{\varepsilon_F} dE E S_{\ell_j}(k; E)$$

- Not** part of fit because it can only make a statement about the two-body contribution

- Result:

- DOM ---> 7.91 MeV/A T/A ---> 22.64 MeV/A
- 10% of particles (momenta > 1.4 fm⁻¹) provide ~²/₃ of the binding energy!
- Exp. 8.55 MeV/A
- Three-body ---> 0.64 MeV/A "attraction" → 1.28 MeV/A "repulsion"
- Argonne GFMC ~ 1.5 MeV/A attraction for three-body <--> Av18

$$E_0^N = \langle \Psi_0^N | \hat{H} | \Psi_0^N \rangle \quad \text{with three-body interaction}$$

$$= \frac{1}{2\pi} \int_{-\infty}^{\varepsilon_F^-} dE \sum_{\alpha, \beta} \{ \langle \alpha | T | \beta \rangle + E \delta_{\alpha, \beta} \} \text{Im} G(\beta, \alpha; E) - \frac{1}{2} \langle \Psi_0^N | \hat{W} | \Psi_0^N \rangle$$

reactions and structure

Do elastic scattering data tell us about correlations?

- Scattering T-matrix

$$\Sigma_{\ell j}(k, k'; E) = \Sigma_{\ell j}^*(k, k'; E) + \int dq q^2 \Sigma_{\ell j}^*(k, q; E) G^{(0)}(q; E) \Sigma_{\ell j}(q, k'; E)$$

- Free propagator

$$G^{(0)}(q; E) = \frac{1}{E - \hbar^2 q^2 / 2m + i\eta}$$

- Propagator

$$G_{\ell j}(k, k'; E) = \frac{\delta(k - k')}{k^2} G^{(0)}(k; E) + G^{(0)}(k; E) \Sigma_{\ell j}(k, k'; E) G^{(0)}(k; E)$$

- Spectral representation

$$G_{\ell j}^p(k, k'; E) = \sum_n \frac{\phi_{\ell j}^{n+}(k) [\phi_{\ell j}^{n+}(k')]^*}{E - E_n^{*A+1} + i\eta} + \sum_c \int_{T_c}^{\infty} dE' \frac{\chi_{\ell j}^{cE'}(k) [\chi_{\ell j}^{cE'}(k')]^*}{E - E' + i\eta}$$

- Spectral density at positive energy

$$S_{\ell j}^p(k, k'; E) = \frac{i}{2\pi} \left[G_{\ell j}^p(k, k'; E^+) - G_{\ell j}^p(k, k'; E^-) \right] = \sum_c \chi_{\ell j}^{cE}(k) [\chi_{\ell j}^{cE}(k')]^*$$

- Coordinate space

$$S_{\ell j}^p(r, r'; E) = \sum_c \chi_{\ell j}^{cE}(r) [\chi_{\ell j}^{cE}(r')]^*$$

- Elastic scattering explicit

$$\chi_{\ell j}^{elE}(r) = \left[\frac{2mk_0}{\pi\hbar^2} \right]^{1/2} \left\{ j_{\ell}(k_0 r) + \int dk k^2 j_{\ell}(kr) G^{(0)}(k; E) \Sigma_{\ell j}(k, k_0; E) \right\}$$

How is it done?

- Solve

$$\Sigma_{\ell j}(k, k'; E) = \Sigma_{\ell j}^*(k, k'; E) + \int dq q^2 \Sigma_{\ell j}^*(k, q; E) G^{(0)}(q; E) \Sigma_{\ell j}(q, k'; E)$$

- with
$$G^{(0)}(q; E) = \frac{1}{E - \hbar^2 q^2 / 2m + i\eta}$$

- See discussion by Arturo Polls
- Note: irreducible self-energy is a complex quantity
- Cross section as shown in first lecture

Elastic nucleon scattering

- Scattering from potential $\langle k_0 | \mathcal{S}^\ell(E) | k_0 \rangle = \left[1 - 2\pi i \left(\frac{mk_0}{\hbar^2} \right) \langle k_0 | \mathcal{T}^\ell(E) | k_0 \rangle \right] \equiv e^{2i\delta_\ell}$
- Potential real \rightarrow phase shift real
- Scattering amplitude
$$f(\theta, \phi) = \sum_l \frac{2l+1}{k_0} \left\{ \frac{-mk_0\pi}{\hbar^2} \right\} \langle k_0 | \mathcal{T}^\ell(E) | k_0 \rangle P_\ell(\cos\theta)$$
$$= \sum_\ell \frac{2\ell+1}{k_0} e^{i\delta_\ell} \sin \delta_\ell P_\ell(\cos\theta)$$
- Elastic nucleon scattering
 - Involves reducible self-energy (see also later)
$$\langle k_0 | \mathcal{S}_{\ell j}(E) | k_0 \rangle \equiv e^{2i\delta_{\ell j}} = 1 - 2\pi i \left(\frac{mk_0}{\hbar^2} \right) \langle k_0 | \Sigma_{\ell j}(E) | k_0 \rangle$$
 - Scattering amplitude
$$f_{m'_s, m_s}(\theta, \phi) = -\frac{4m\pi^2}{\hbar^2} \langle \mathbf{k}' m'_s | \Sigma(E) | \mathbf{k} m_s \rangle$$
 - Phase shift now includes imaginary part when potential is absorptive

Spin-orbit physics included

- Scattering amplitude $f_{m'_s, m_s}(\theta, \phi) = -\frac{4m\pi^2}{\hbar^2} \langle \mathbf{k}' m'_s | \Sigma(E) | \mathbf{k} m_s \rangle$

- Rewrite $[f(\theta, \phi)] = \mathcal{F}(\theta)I + \boldsymbol{\sigma} \cdot \hat{\mathbf{n}}\mathcal{G}(\theta)$

- with $\hat{\mathbf{n}} = \frac{\mathbf{k} \times \mathbf{k}'}{|\mathbf{k} \times \mathbf{k}'|} = \frac{\hat{\mathbf{k}} \times \hat{\mathbf{k}'}}{\sin \theta}$

- then

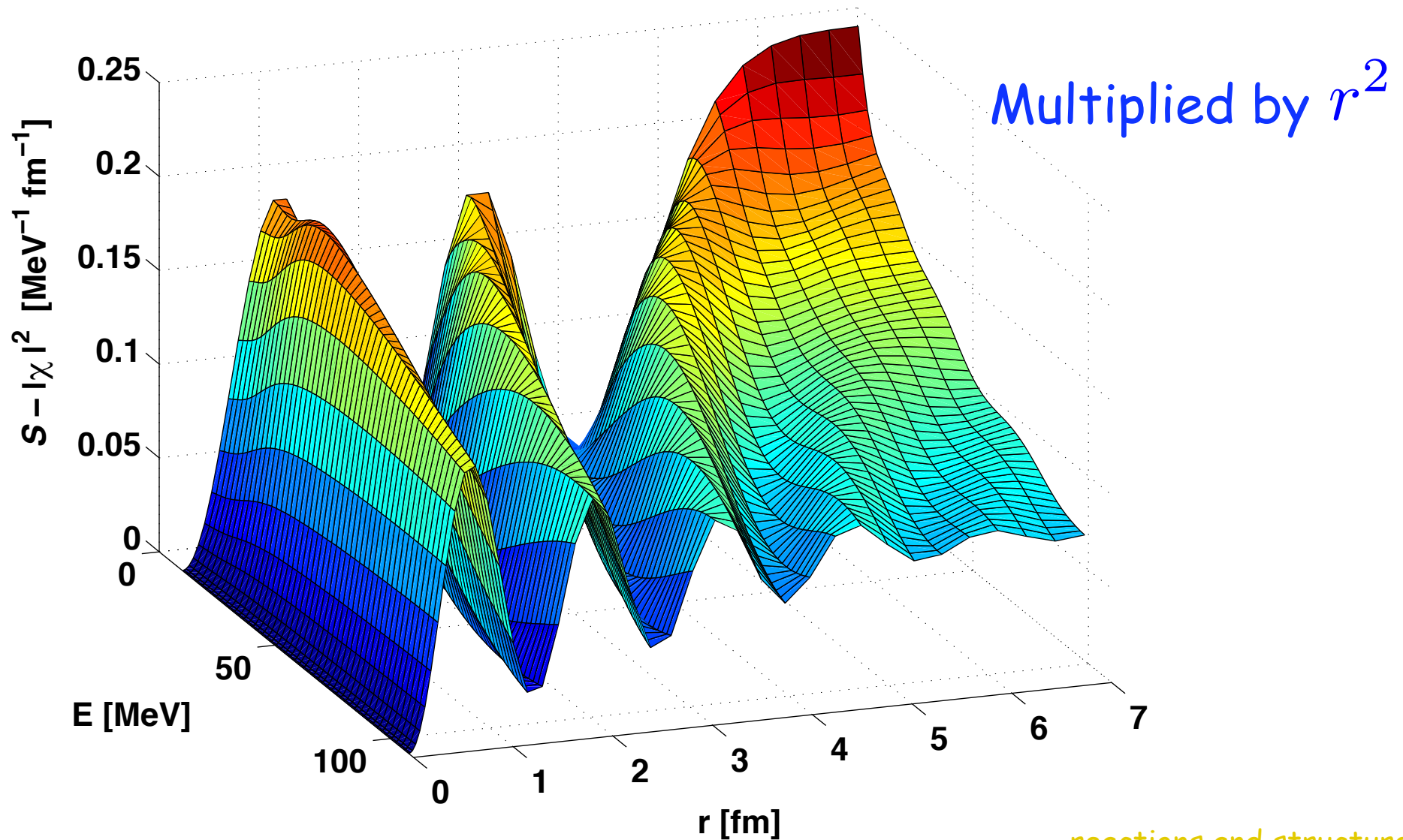
$$\mathcal{F}(\theta) = \frac{1}{2ik} \sum_{\ell=0}^{\infty} [(\ell+1) \{e^{2i\delta_{\ell+}} - 1\} + \ell \{e^{2i\delta_{\ell-}} - 1\}] P_{\ell}(\cos \theta)$$

$$\mathcal{G}(\theta) = \frac{\sin \theta}{2k} \sum_{\ell=1}^{\infty} [e^{2i\delta_{\ell+}} - e^{2i\delta_{\ell-}}] P'_{\ell}(\cos \theta)$$

- Unpolarized differential cross section $\left(\frac{d\sigma}{d\Omega}\right)_{unpol} = |\mathcal{F}|^2 + |\mathcal{G}|^2$

Adding an $s_{1/2}$ neutron to ^{40}Ca

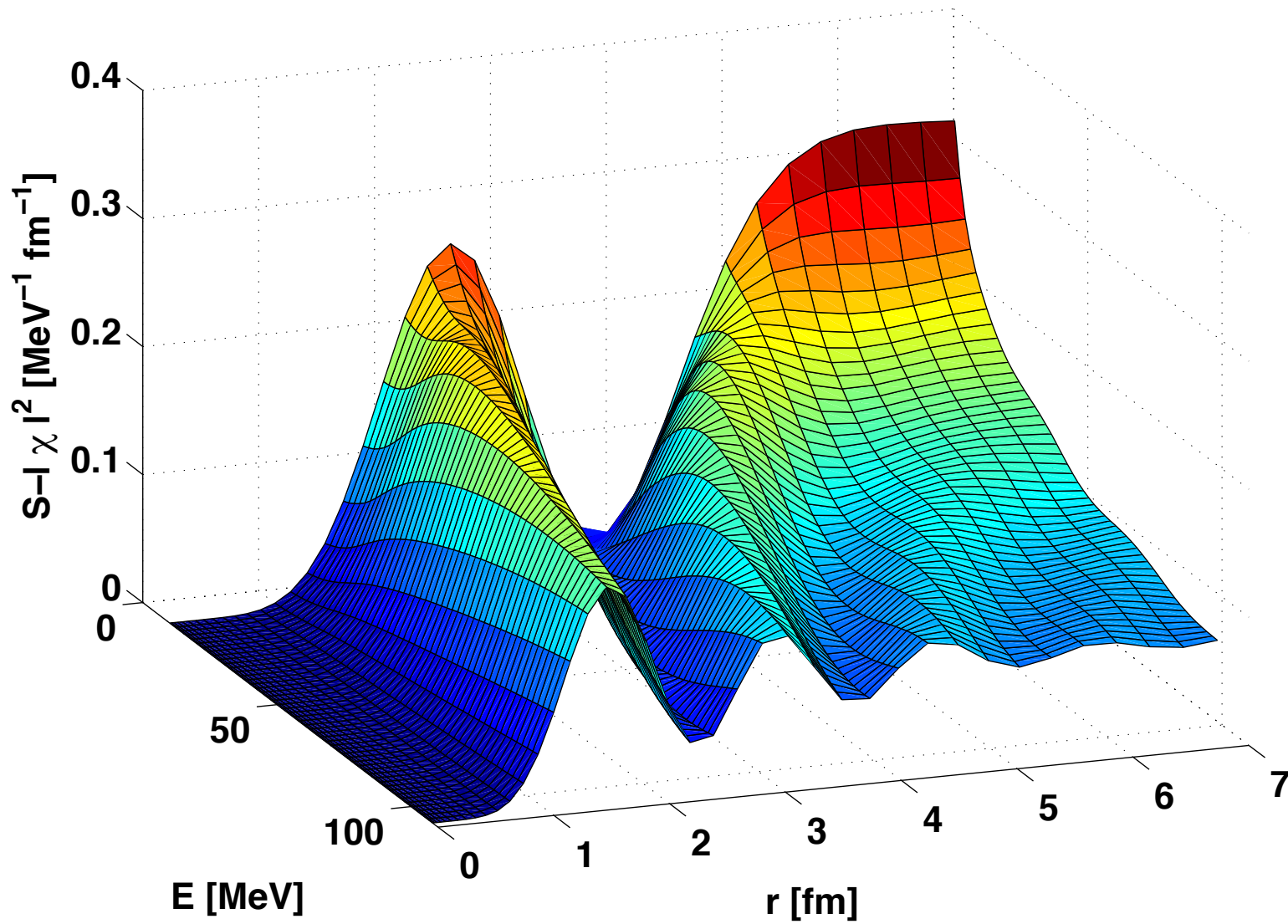
- Inelastically!
- Zero when there is no absorption!



$d_{3/2}$

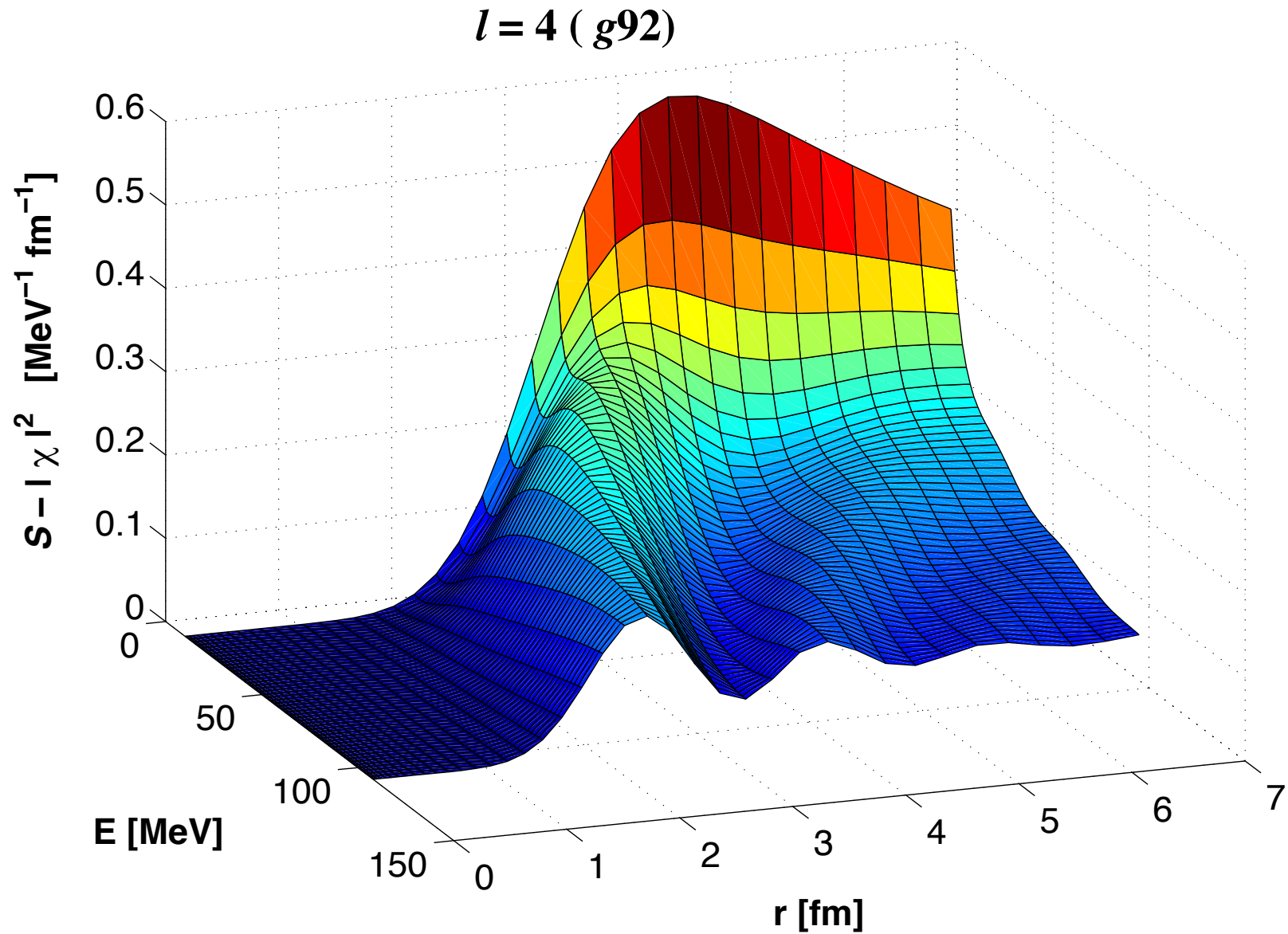
$l=2$

- One node now



No nodes

- Asymptotically determined by inelasticity



Determine location of bound-state strength

- Fold spectral function with bound state wave function

$$S_{\ell j}^{n+}(E) = \int dr r^2 \int dr' r'^2 \phi_{\ell j}^{n-}(r) S_{\ell j}^p(r, r'; E) \phi_{\ell j}^{n-}(r')$$

- → Addition probability of bound orbit
- Also removal probability

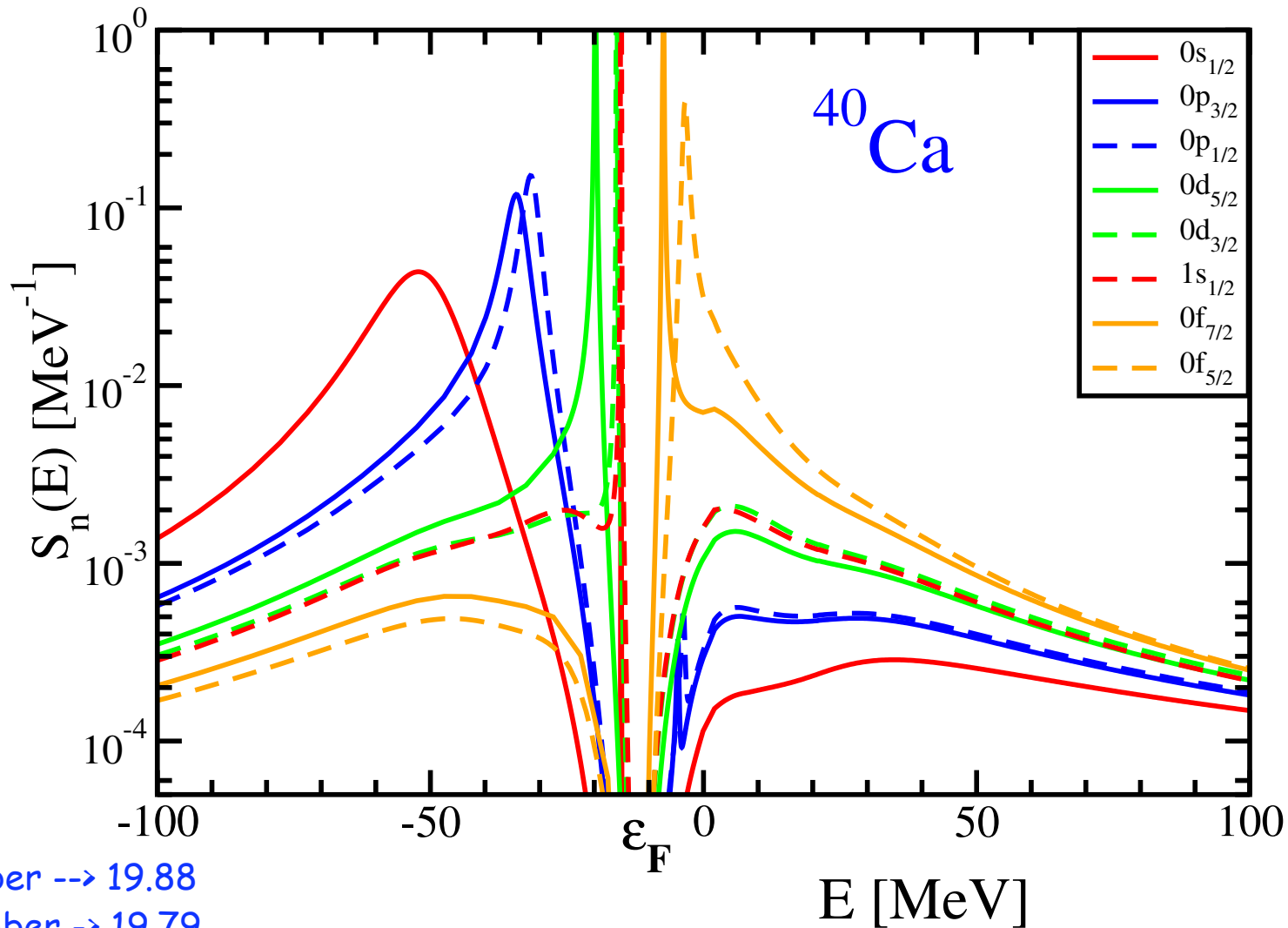
$$S_{\ell j}^{n-}(E) = \int dr r^2 \int dr' r'^2 \phi_{\ell j}^{n-}(r) S_{\ell j}^h(r, r'; E) \phi_{\ell j}^{n-}(r')$$

- Overlap function $\sqrt{S_{\ell j}^n} \phi_{\ell j}^{n-}(r) = \langle \Psi_n^{A-1} | a_{r\ell j} | \Psi_0^A \rangle$

- Sum rule $1 = n_{n\ell j} + d_{n\ell j} = \int_{-\infty}^{\epsilon_F} dE S_{\ell j}^{n-}(E) + \int_{\epsilon_F}^{\infty} dE S_{\ell j}^{n+}(E)$

Spectral function for bound states

- [0,200] MeV → constrained by elastic scattering data



proton number --> 19.88

neutron number -> 19.79

$S_{0d_{3/2}} = 0.76$

$S_{1s_{1/2}} = 0.78$

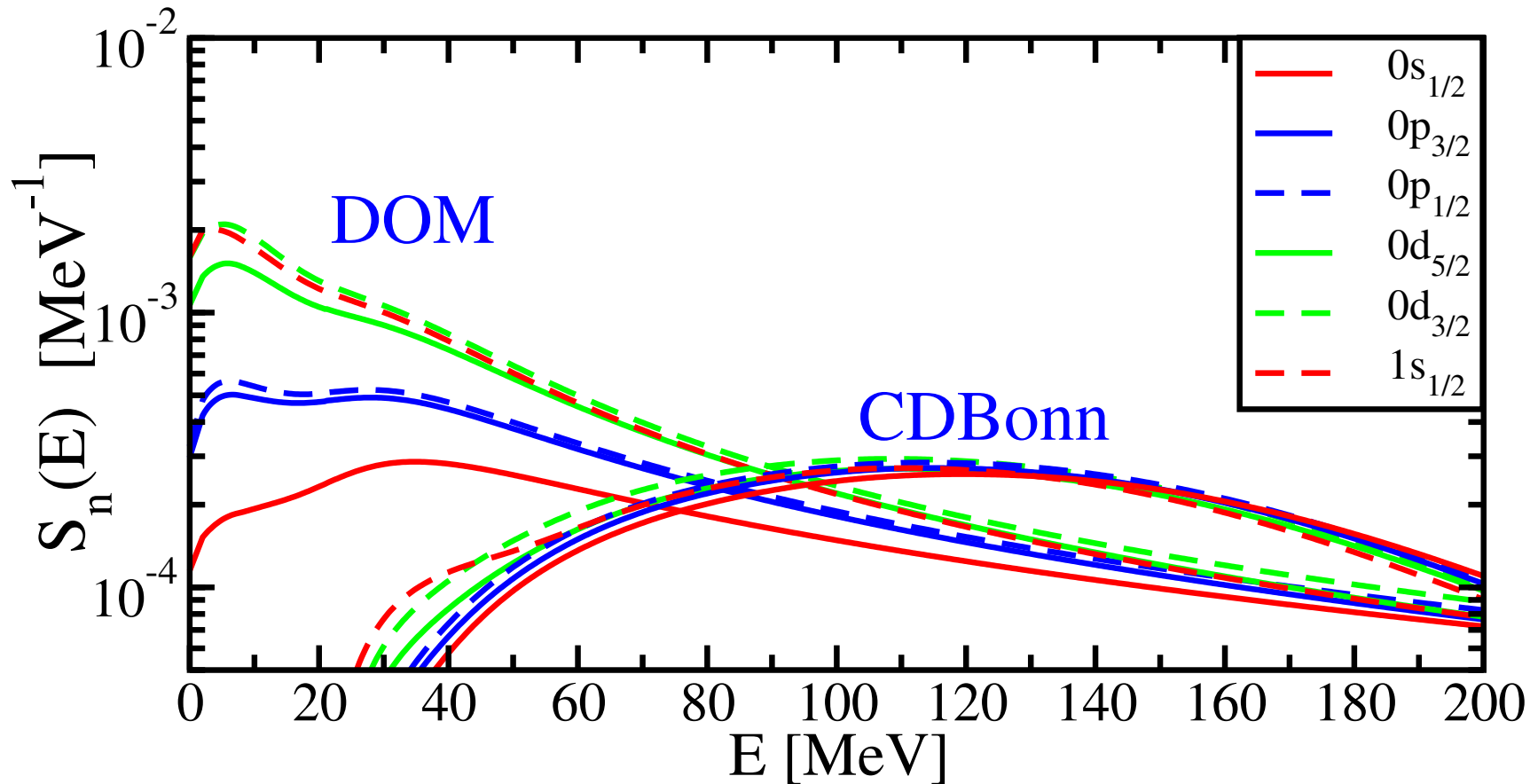
0.15 larger than NIKHEF analysis!

PRC90, 061603(R) (2014)

reactions and structure

Compared with ab initio \rightarrow SRC only

- CDBonn probably too soft
- SRC relevant at higher energy



Quantitatively

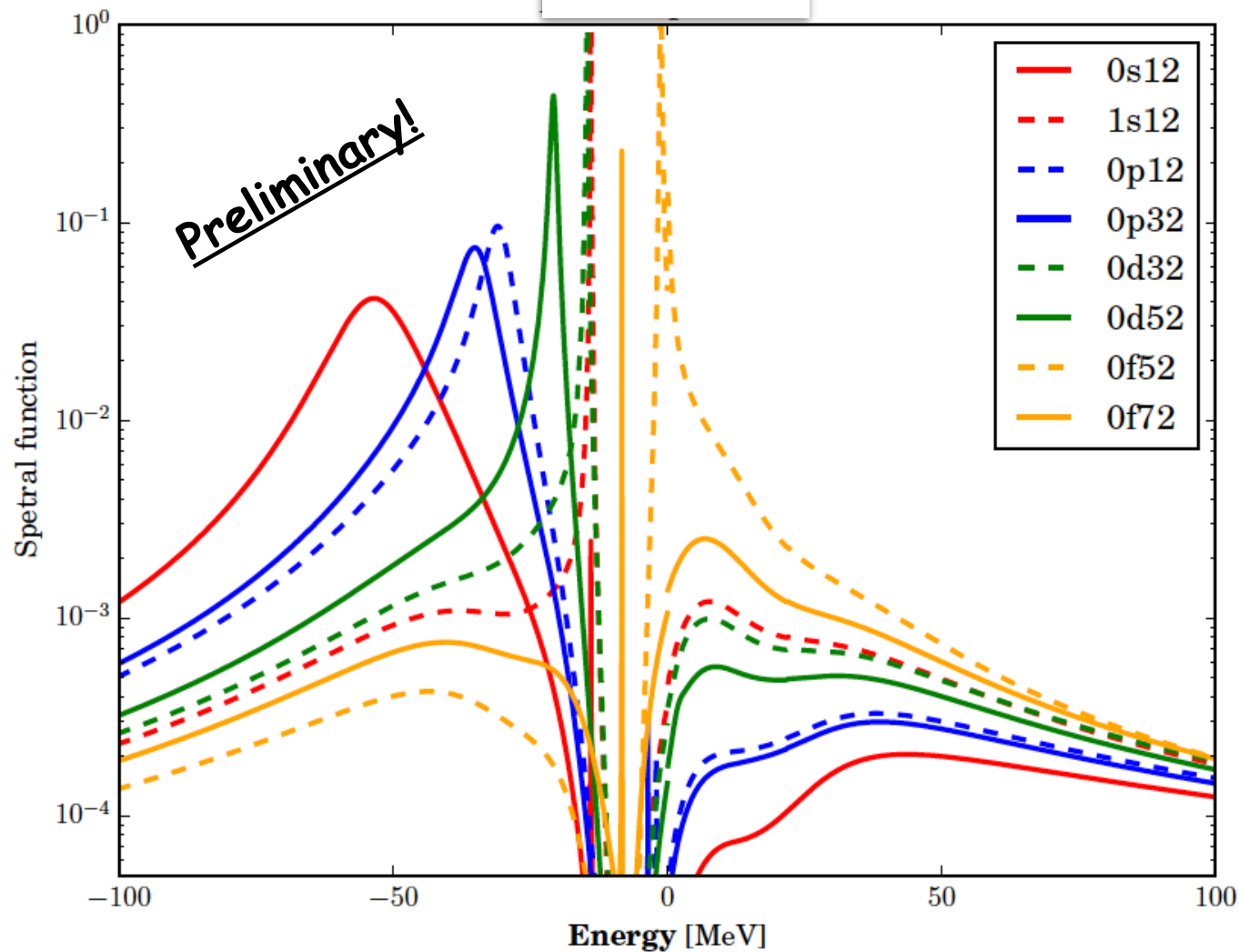
- Orbit closer to the continuum → more strength in the continuum
- Note “particle” orbits
- Drip-line nuclei have valence orbits very near the continuum

Table 1: Occupation and depletion numbers for bound orbits in ^{40}Ca . $d_{nlj}[0, 200]$ depletion numbers have been integrated from 0 to 200 MeV. The fraction of the sum rule that is exhausted, is illustrated by $n_{nlj} + d_{nlj}[\varepsilon_F, 200]$. Last column $d_{nlj}[0, 200]$ depletion numbers for the CDBonn calculation.

orbit	n_{nlj} DOM	$d_{nlj}[0, 200]$ DOM	$n_{nlj} + d_{nlj}[\varepsilon_F, 200]$ DOM	$d_{nlj}[0, 200]$ CDBonn
$0s_{1/2}$	0.926	0.032	0.958	0.035
$0p_{3/2}$	0.914	0.047	0.961	0.036
$1p_{1/2}$	0.906	0.051	0.957	0.038
$0d_{5/2}$	0.883	0.081	0.964	0.040
$1s_{1/2}$	0.871	0.091	0.962	0.038
$0d_{3/2}$	0.859	0.097	0.966	0.041
$0f_{7/2}$	0.046	0.202	0.970	0.034
$0f_{5/2}$	0.036	0.320	0.947	0.036

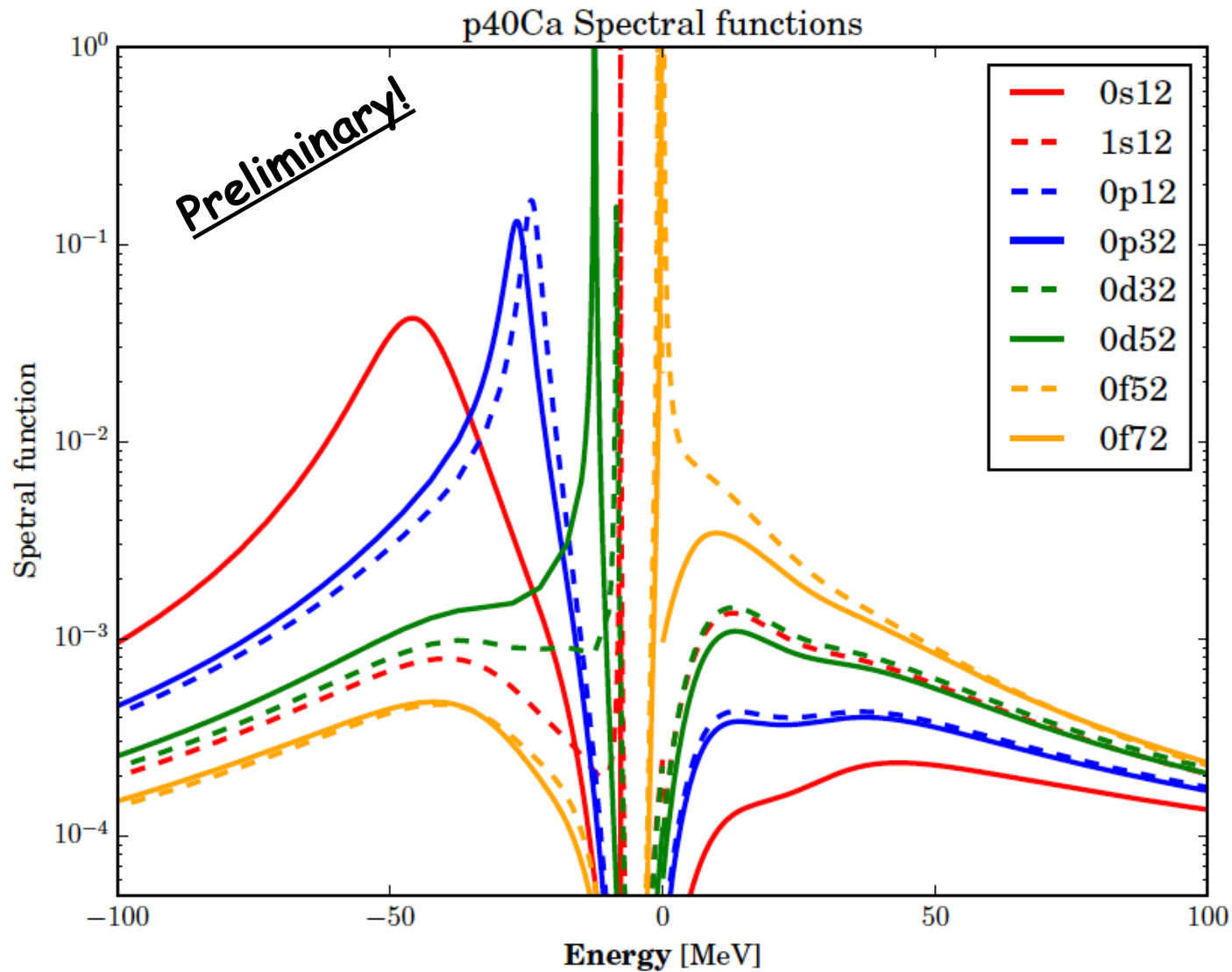
Neutron spectral function in ^{48}Ca

- Neutrons in ^{48}Ca less correlated \leftrightarrow ^{40}Ca but qualitatively similar



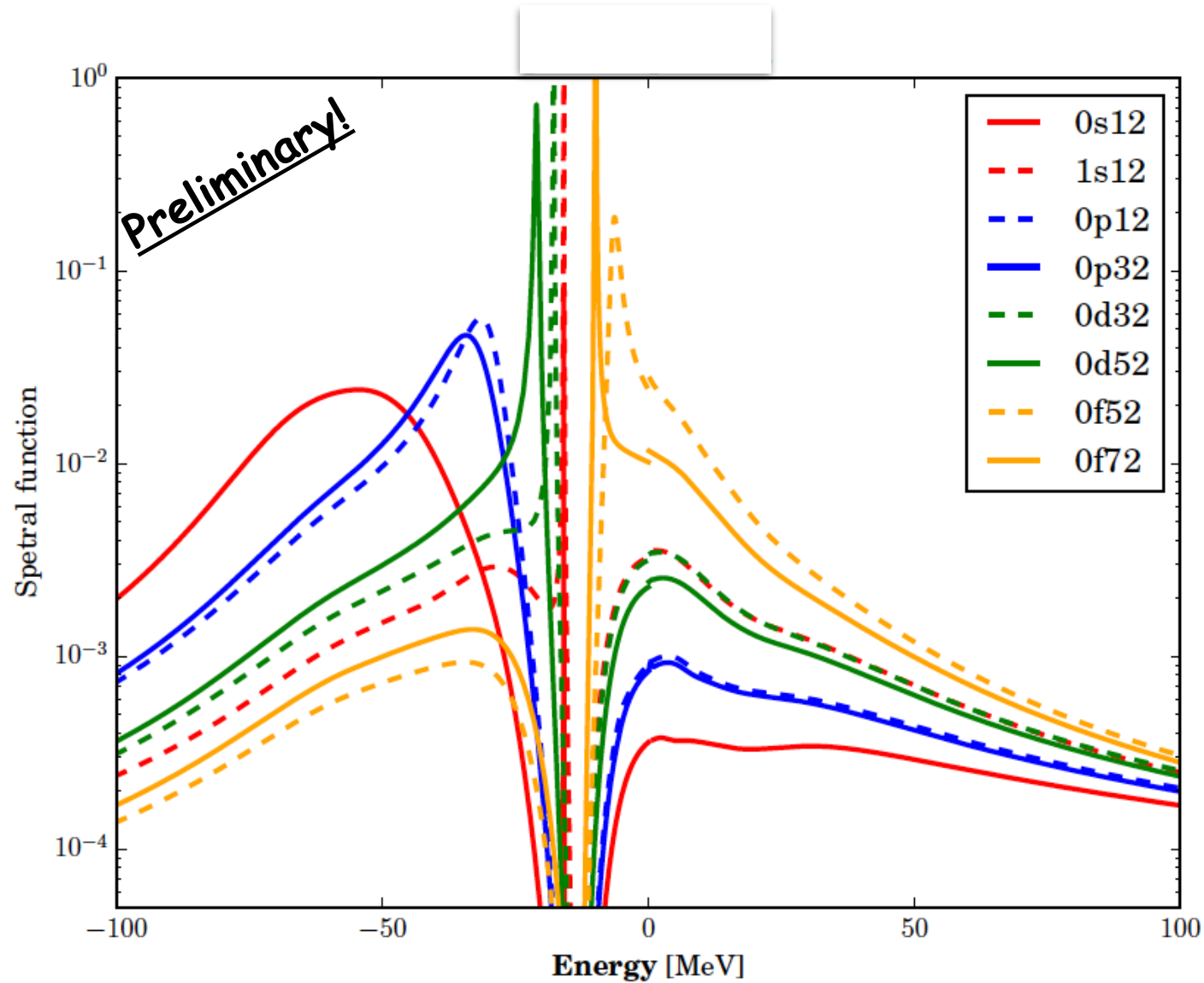
Proton spectral function in ^{40}Ca

- Learning how to deal with Coulomb in momentum space



Protons in ^{48}Ca

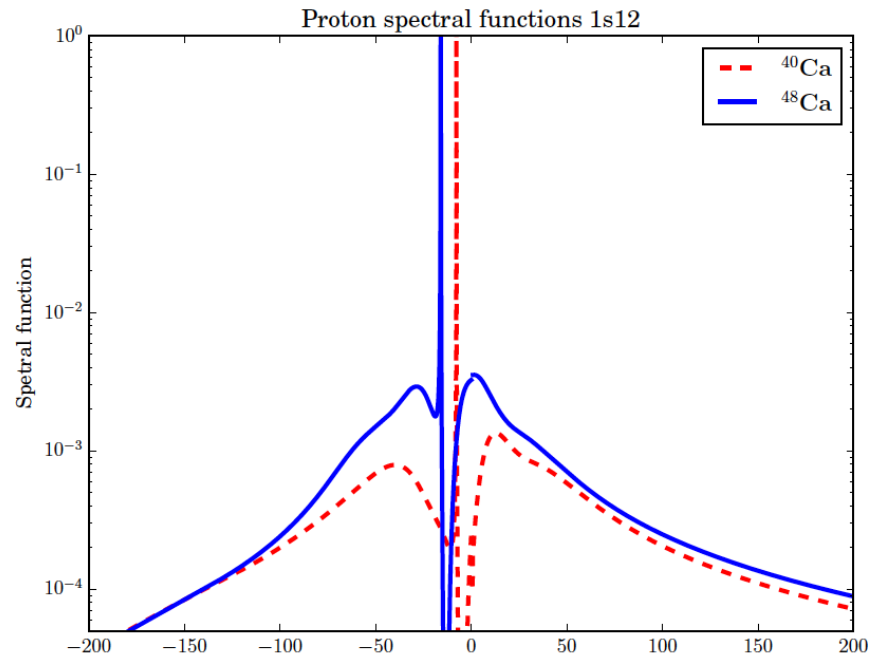
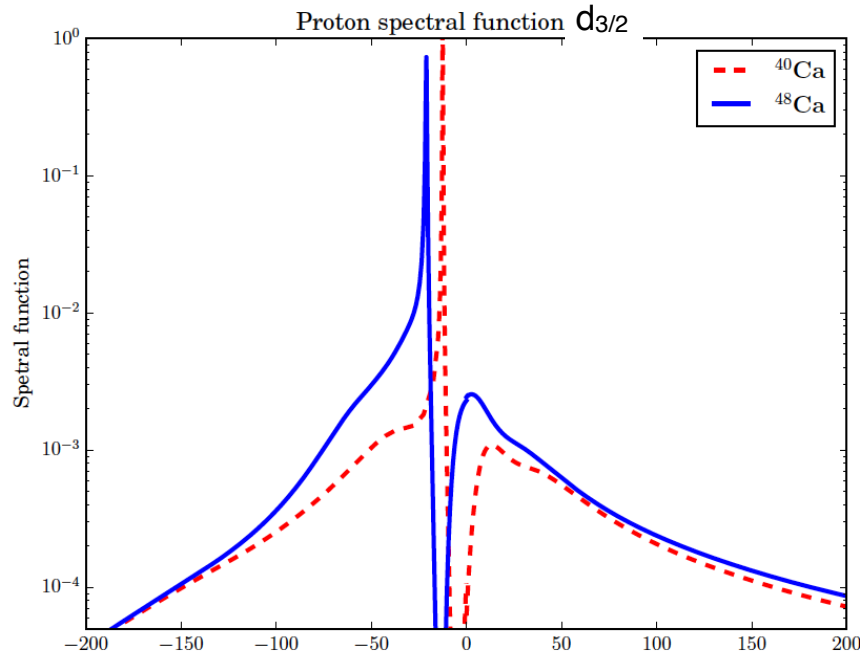
- Protons in ^{48}Ca more correlated than in ^{40}Ca



Quantitative comparison of ^{40}Ca and ^{48}Ca

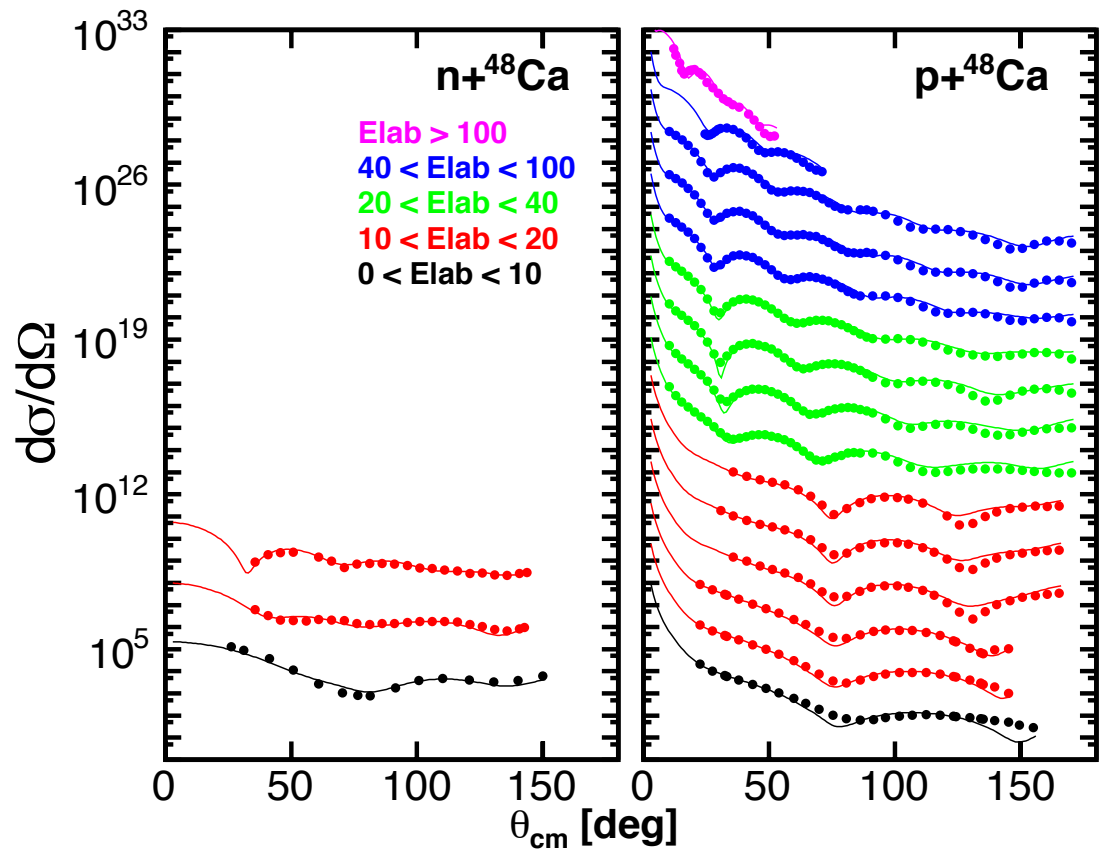
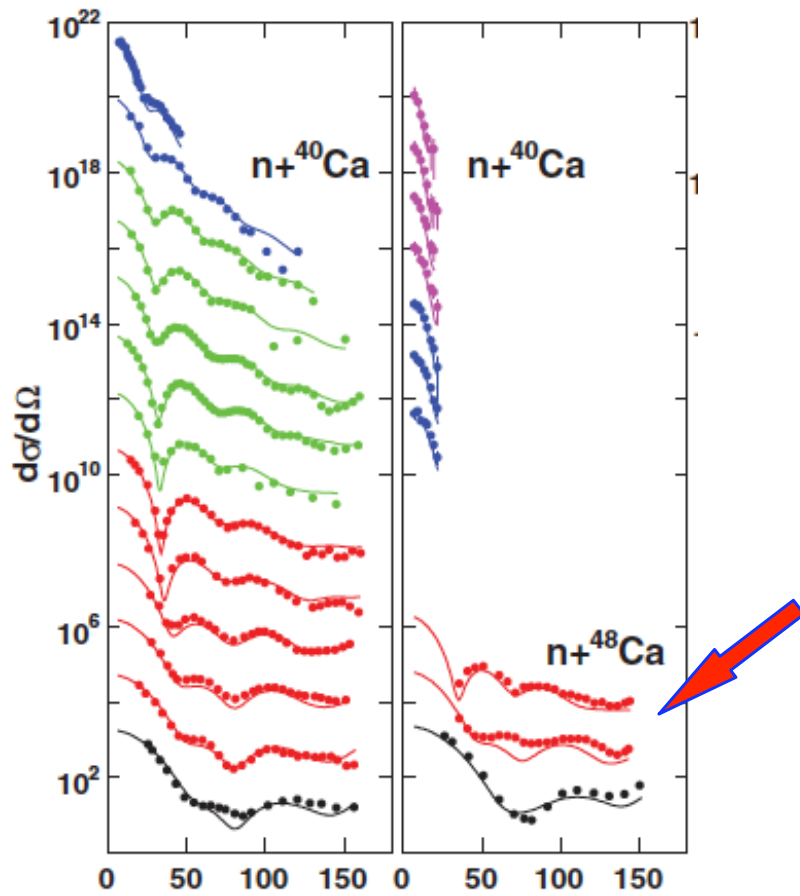
Spectroscopic factors	^{40}Ca	p ^{48}Ca	n ^{48}Ca
$0d_{3/2}$	0.76	0.65 ↓	0.80 ↑
$1s_{1/2}$	0.78	0.71 ↓	0.83 ↑
$0f_{7/2}$	0.73	0.59 ↓	0.84 ↑

Comparison for $d_{3/2}$ and $s_{1/2}$ protons



In progress

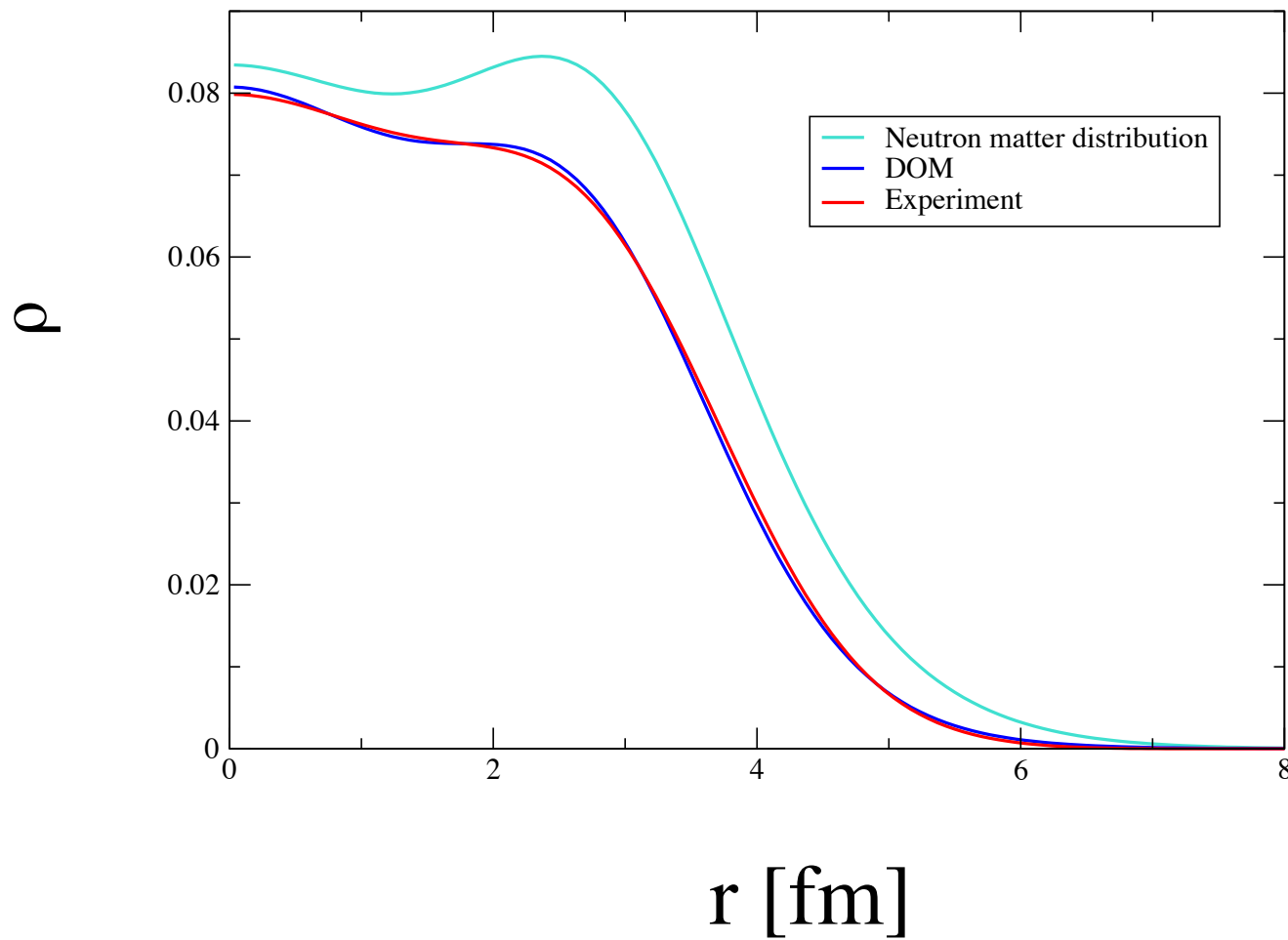
- ^{48}Ca \rightarrow charge density has been measured
- Recent neutron elastic scattering **data** \rightarrow PRC83,064605(2011)
- Local DOM **OLD** Nonlocal DOM **NEW**



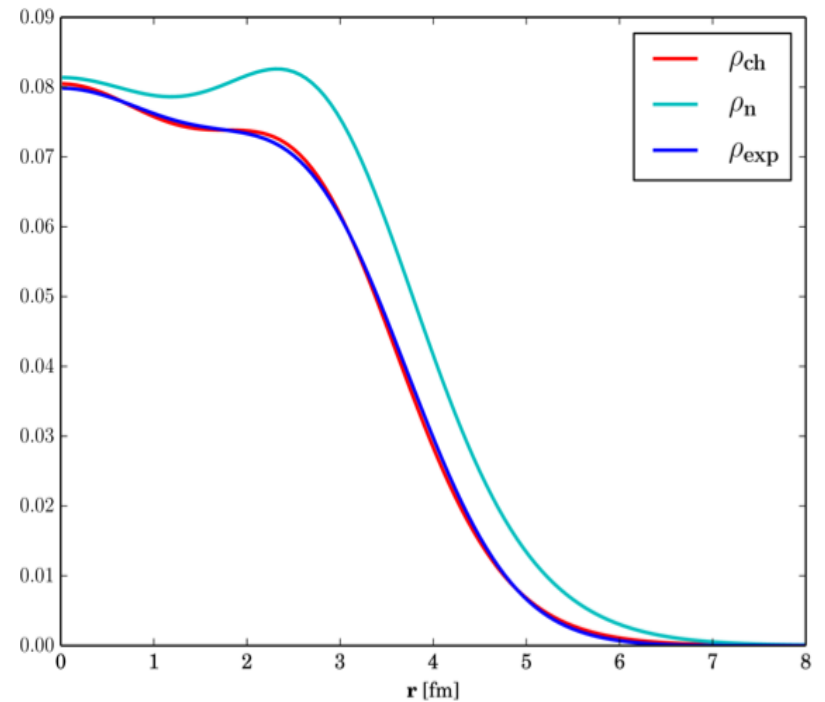
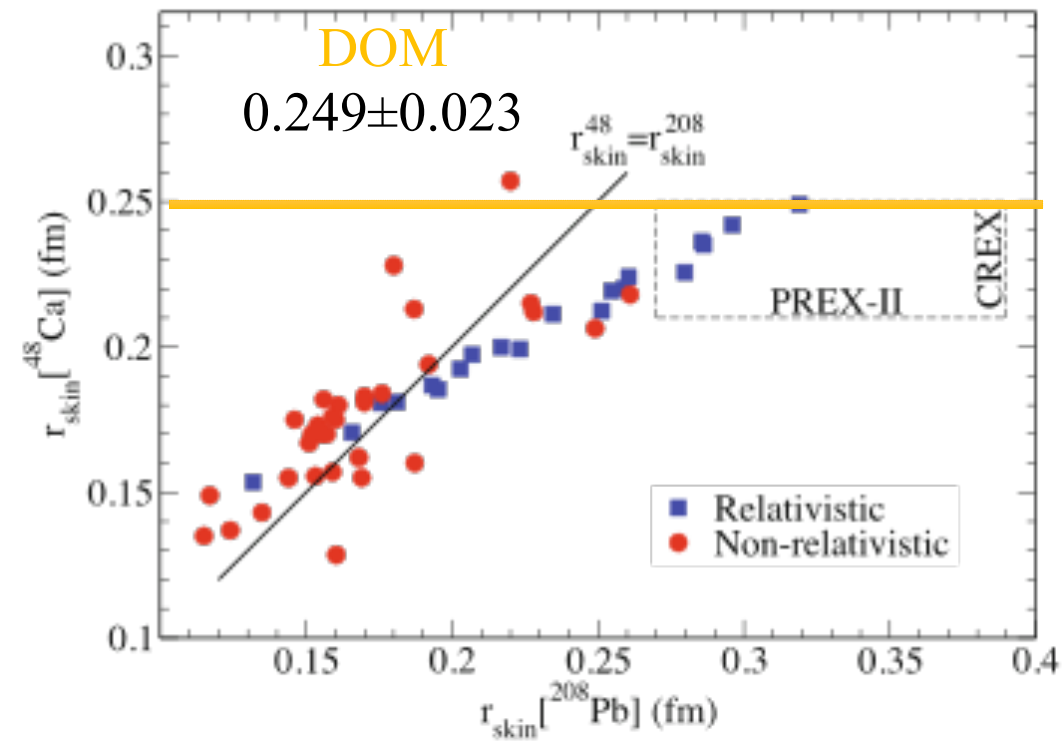
Results for ^{48}Ca

- Density distributions
- DOM \rightarrow neutron distribution $\rightarrow R_n - R_p$

^{48}Ca nuclear charge distribution



^{48}Ca Densities



Eur. Phys. J. A (2014)
C.J. Horowitz, K.S. Kumar, and R.
Michaels

$R_n - R_p$ for ^{48}Ca

- Charge density for ^{40}Ca ✓
- Charge density for ^{48}Ca ✓
- Neutrons in ^{40}Ca well constrained ✓
- 8 extra neutrons in ^{48}Ca constrained by new elastic scattering data at low energy and total cross sections up to 200 MeV, level structure, and particle number ✓
- neutron skin "large"
- neutron distribution smooth like the charge density ✓

Question

- How important is the "straightjacket effect" for the relation between the slope of the symmetry energy and $R_n - R_p$?

Neutron Skin of ^{208}Pb , Nuclear Symmetry Energy, and the Parity Radius Experiment

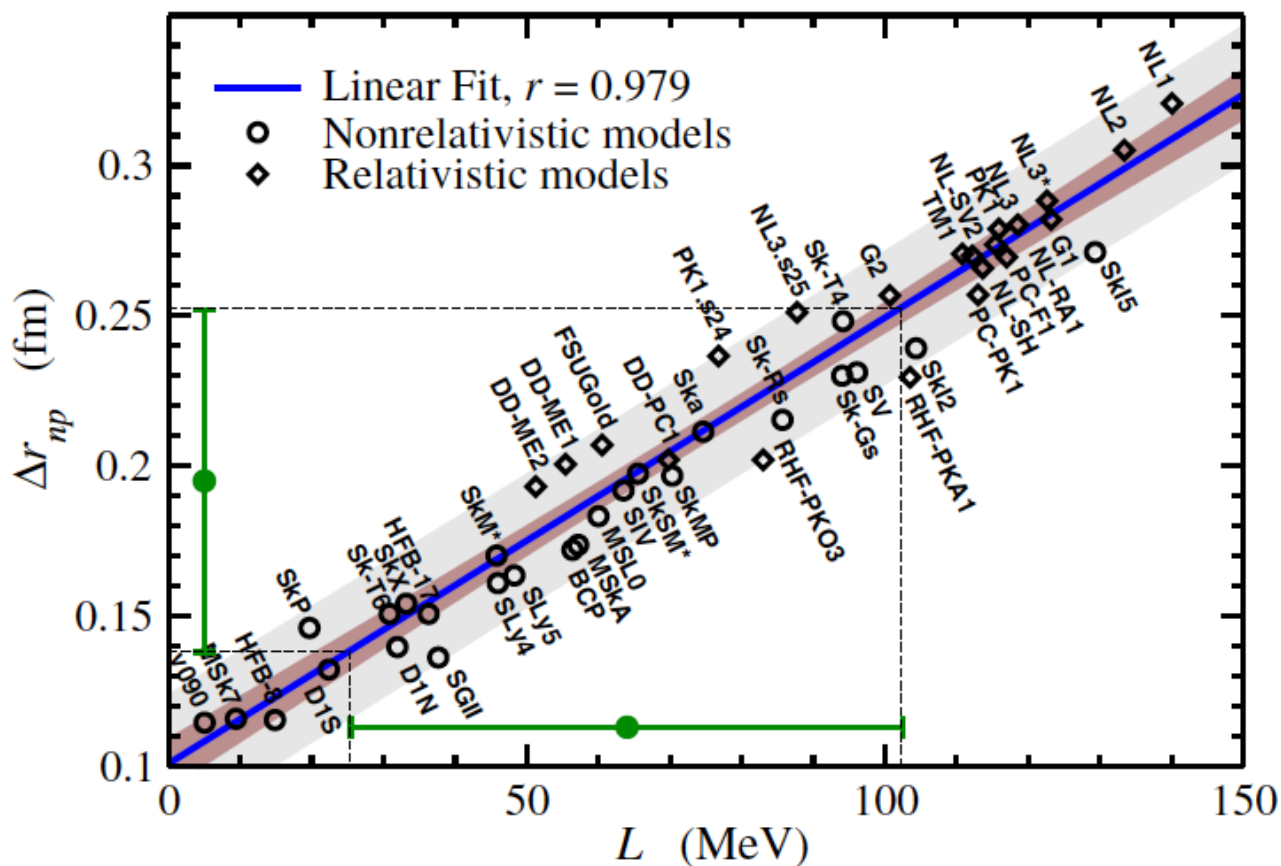
X. Roca-Maza,^{1,2} M. Centelles,¹ X. Viñas,¹ and M. Warda³

¹Departament d'Estructura i Constituents de la Matèria and Institut de Ciències del Cosmos, Facultat de Física, Universitat de Barcelona, Diagonal 647, 08028 Barcelona, Spain

²INFN, sezione di Milano, via Celoria 16, I-20133 Milano, Italy

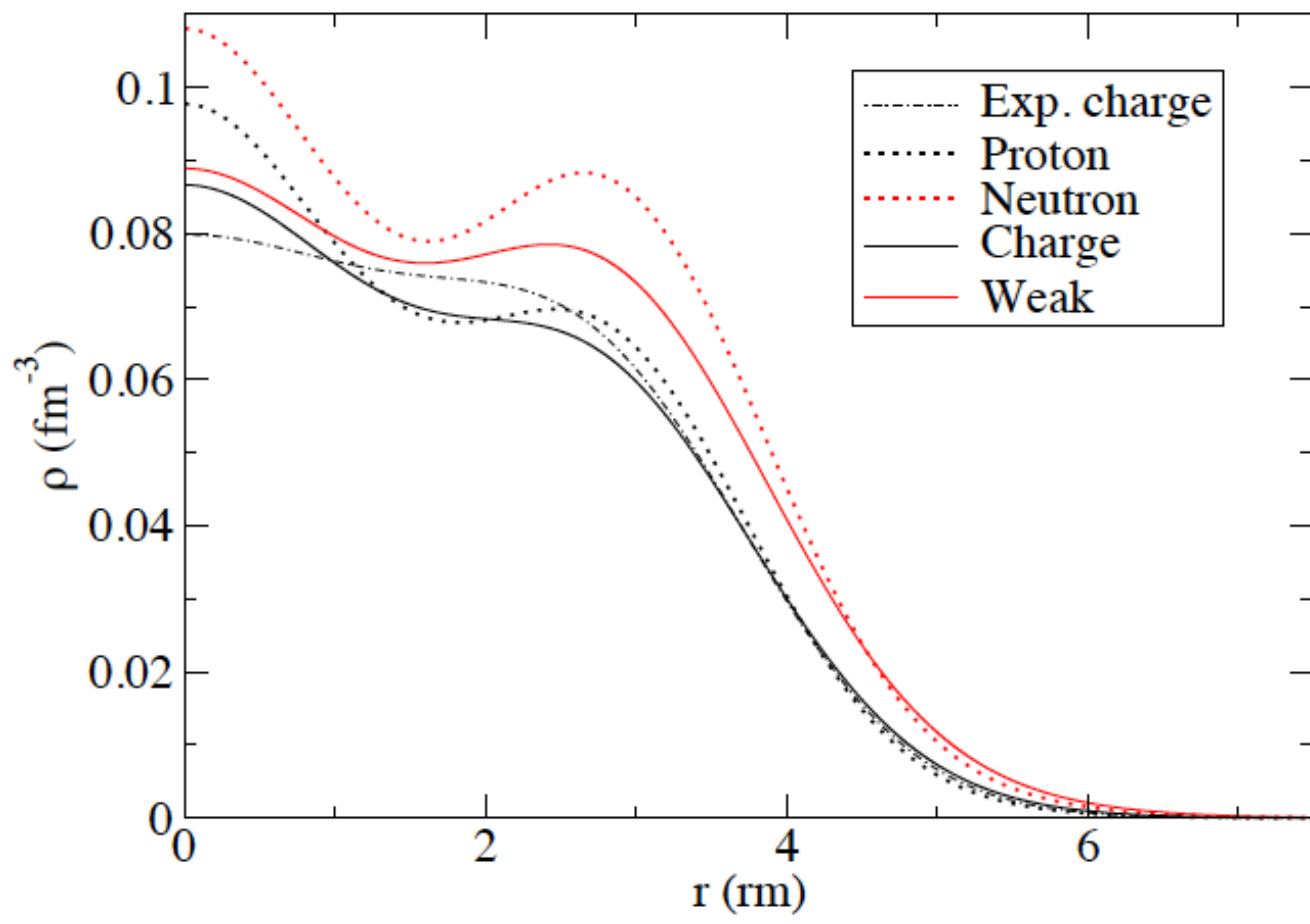
³Katedra Fizyki Teoretycznej, Uniwersytet Marii Curie-Skłodowskiej, ul. Radziszewskiego 10, 20-031 Lublin, Poland

(Received 7 March 2011; published 21 June 2011)



Hagen et al. based on PRL109,032502(2012)

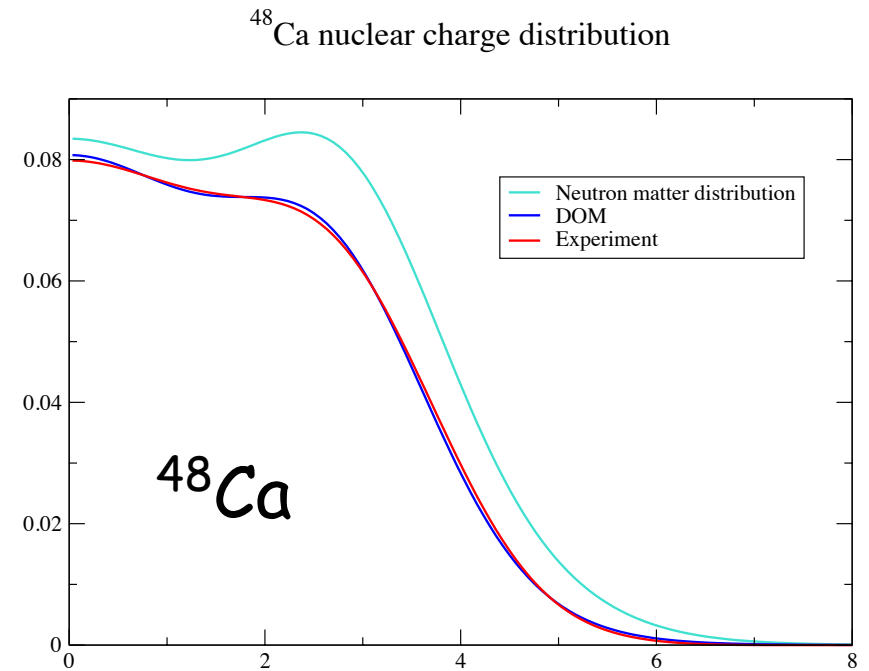
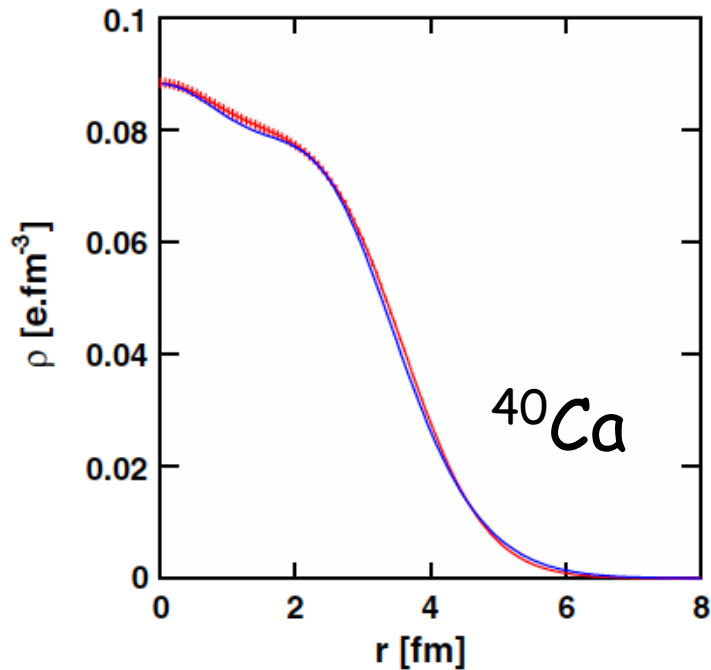
- Coupled-cluster ab initio
- Chiral forces have limitations
- Coupled-cluster method also
- ^{48}Ca



R_p	3.438
R_n	3.594
$R_n - R_p$	0.156
R_W	3.697
R_{ch}	3.526
R_{ch} (exp)	3.48

Can we get L from the DOM?

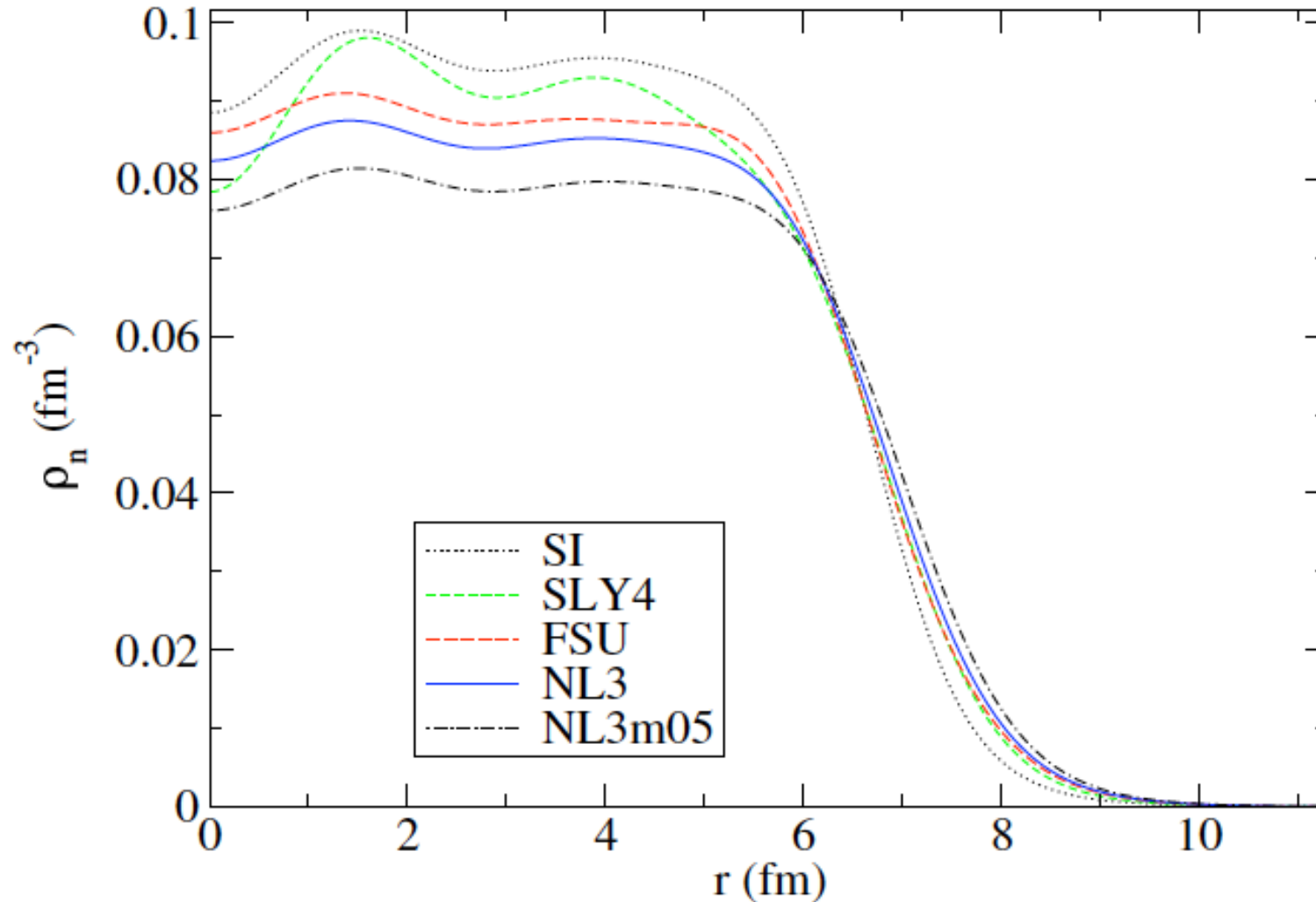
- Perhaps...



- We could calculate energy density as a function of r for both nuclei...
- Identify the normal density part from the interior...

Mean-field for ^{208}Pb neutrons

B. Shufang, C J Horowitz and R Michaels *J. Phys. G: Nucl. Part. Phys.* 39 (2012) 015104

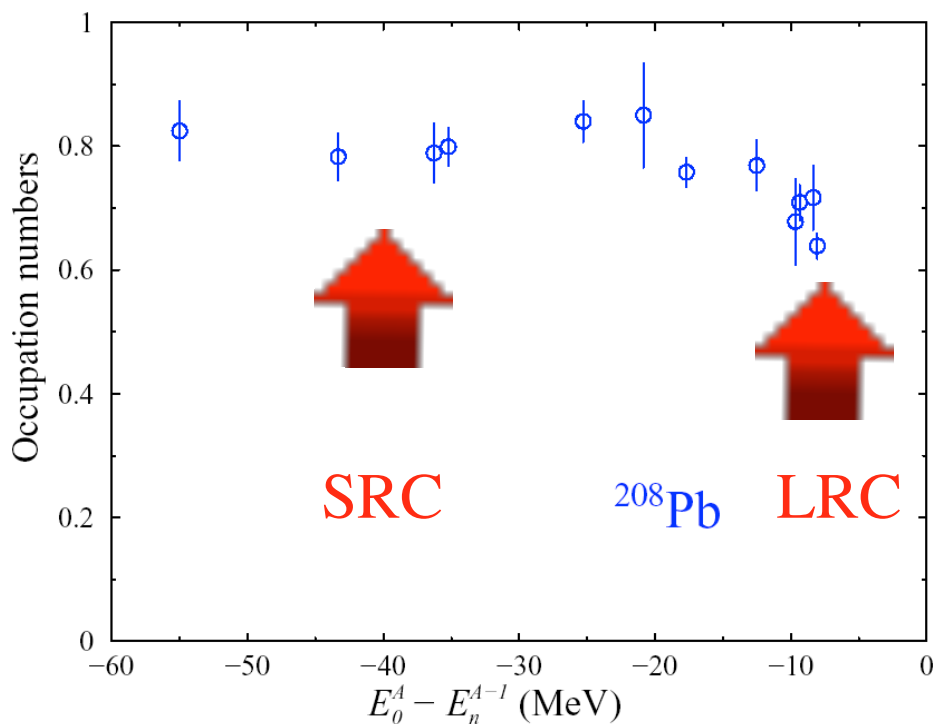


Conclusions

- It **is** possible to link nuclear reactions and nuclear structure
- Vehicle: nonlocal version of **Dispersive Optical Model** (Green's function method) pioneered by Mahaux → **DSM**
- Can be used as input for analyzing nuclear reactions
- Can predict properties of exotic nuclei
- "Benchmark" for ab initio calculations: e.g. V_{NNN} → binding
- Can describe ground-state properties
 - charge density & momentum distribution
 - spectral properties including high-momentum Jefferson Lab data
- **Elastic scattering determines depletion of bound orbitals**
- **Outlook:** reanalyze many reactions with nonlocal potentials...
- For $N \geq Z$ exhibits sensitivity to properties of neutrons → weak charge → **neutron skin and perhaps more** reactions and structure

M. van Batenburg & L. Lapikás from $^{208}\text{Pb} (e, e' p) ^{207}\text{Tl}$
 NIKHEF 2001 data (one of the last experiments)

Occupation of deeply-bound proton levels from EXPERIMENT



Up to 100 MeV missing energy and
 270 MeV/c missing momentum

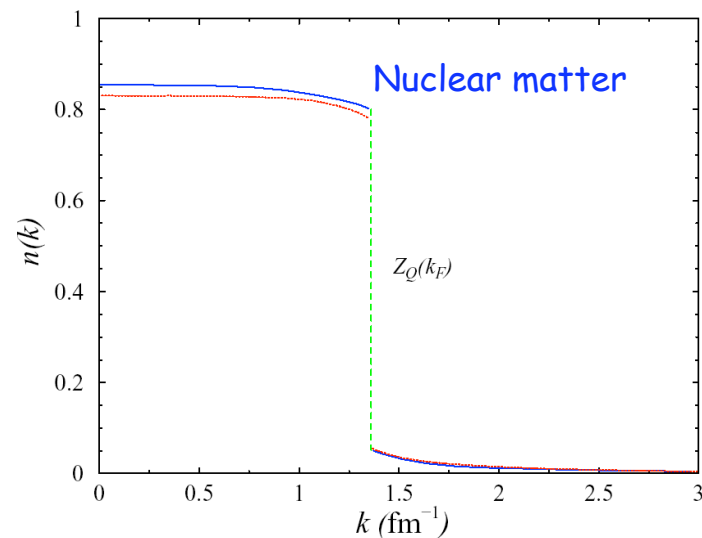
Covers the **whole mean-field domain!!**

Confirms predictions for depletion

$n(0) \Rightarrow$ 0.85 Reid

0.87 Argonne V18

0.89 CDBonn/N3LO



reactions and structure